Journal of Medicinal Chemistry

Article

Discovery of Janus Kinase 2 (JAK2) and Histone Deacetylase (HDAC) Dual Inhibitors as a Novel Strategy for Combinational Treatment of Leukemia and Invasive Fungal Infections

Yahui Huang, Guoqiang Dong, Huanqiu Li, Na Liu, Wannian Zhang, and Chunquan Sheng

J. Med. Chem., **Just Accepted Manuscript** • DOI: 10.1021/acs.jmedchem.8b00393 • Publication Date (Web): 25 Jun 2018

ACS Publications

is published by the American Chemical Society. 1155 Sixteenth Street N.W., Washington, DC 20036

Discovery of Janus Kinase 2 (JAK2) and Histone Deacetylase (HDAC) Dual Inhibitors as a Novel Strategy for Combinational Treatment of Leukemia and Invasive Fungal Infections

Yahui Huang[1,†], Guoqiang Dong[1,†], Huanqiu Li[2,†], Na Liu[1], Wannian Zhang[1], Chunquan Sheng[1,*]

[1]*School of Pharmacy, Second Military Medical University, 325 Guohe Road, Shanghai 200433, People's Republic of China*

[2] *College of Pharmaceutical Science, Soochow University, Suzhou 215123, PR China*

ABSTRACT

Clinically, leukemia patients often suffer from limited efficacy of chemotherapy and high risks to be infected by invasive fungal pathogens. Herein a novel therapeutic strategy was developed that a small molecule can simultaneously treat leukemia and invasive fungal infections (IFIs). Novel Janus kinase 2 (JAK2) and histone deacetylase (HDAC) dual inhibitors were identified to possess potent antiproliferative activity toward hematological cell lines and excellent synergistic effects with flcuonazole to treat resistant *Candida albicans* infections. In particular, compound **20a**, a highly active and selective JAK2/HDAC6 dual inhibitor, showed excellent *in vivo* antitumor efficacy in several acute myeloid leukemia (AML) models, and synergized with fluconazole for the treatment of resistant *Candida albicans* infections. This study highlights the therapeutic potential of JAK2/HDAC dual inhibitors in treating AML and IFIs and provides an efficient strategy for multi-targeting drug discovery.

INTRODUCTION

Invasive fungal infections (IFIs) are life-threatening and often occur in immunocompromised hosts. Leukemia patients undergoing chemotherapy, hematopoietic stem cell transplantation (HSCT) or immunosuppressive therapy are highly vulnerable to IFIs.[1] According to NCCN guidelines (national comprehensive cancer network clinical practice guidelines in oncology), primary antifungal prophylaxis (azoles, amphotericin B or echinocandins) should be used in high-risk patients, especially those with acute myeloid leukemia (AML) and graft versus host disease (GVHD). However, severe drug resistance has been observed for antifungal agents. In recipients of HSCT, the mortality associated with IFIs still remains high. Tyrosine kinase inhibitors have been widely used in the targeted therapy of leukemia.[2] Despite the success, clinically available therapeutics generally suffered from limited efficacy and drug resistance. Thus, the development new generation of kinase inhibitors for targeted therapy remains an active research area. Especially, a kinase inhibitor that can synergize with antifungal agents and improve their potency to treat resistant IFIs is highly desirable. However, the discovery of such a di-functional molecule is challenging.

The Janus kinases (JAK1, JAK2, JAK3, and TYK2) belong to the family of intracellular protein tyrosine kinases, which play essential roles in the signaling of a variety of cytokines.[3] Activation of JAKs by different cytokines results in phosphorylation and dimerization of the STAT (signal transducers and activators of transcription) proteins, which further translocate to the nucleus and activate gene

transcription.[4] The JAK/STAT signaling axis is associated with diverse biological functions including inflammation, immune function and hematopoiesis.[5, 6] JAK inhibitors have been extensively investigated as new therapeutics for the treatment of immune-inflammatory diseases (*e.g.* rheumatoid arthritis, RA) and cancer (*e.g.* leukemia, lymphoma and solid tumor).[6-8] Currently, a number of pan-JAK and selective JAK inhibitors have been discovered.[6] Pan-JAK inhibitor tofacitinib[9] was approved for the treatment of RA, and JAK1/2 inhibitor ruxolitinib (**Figure 1**)[10] was marketed to treat myelofibrosis and polycythemia vera. Among the four JAK subtypes, JAK2 was proven to be critical for the growth and progression tumor. JAK2 inhibitors have been evaluated in clinical trials for the treatment of a wide spectrum of hematological malignancies as well as solid tumors.[11] However, resistance of JAK2 inhibitors has been observed.[12, 13] To improve the therapeutic effects and reduce the risk of resistance, combinational drug therapy[14-16] or development of JAK2-based multi-targeting antitumor agents[17, 18] offered new opportunities.

As a family of epigenetic enzymes, histone deacetylases (HDACs) remove acetyl groups from lysine on histones and other proteins, which play an essential role on various cellular functions including gene regulation, transcription, and cell proliferation, differentiation and death. Overexpression of HDACs are observed in different human cancers, and thus they are regarded as promising antitumor drug targets.[19] Up to date, four HDAC inhibitors, namely vorinostat (SAHA, **2**), romidepsin, belinostat and panobinostat, have been approved for the treatment of hematologic cancer.[20-23] Similar to JAK2, HDAC-based multi-targeting antitumor

agents have achieved great success in achieving higher efficacy, broader antitumor spectrum and better safety profiles.[24]

Clinically, specific drug combinations have been widely used in cancer therapy. However, drug cocktails often suffer from complicated dose (or schedule) design as well as poor patient compliance.[25] In contrast, a single multi-targeting molecule has obvious advantages in terms of synergistic antitumor effects, more predictable and favorable pharmacokinetic (PK) profiles, reduced compliance difficulties and drug-drug interactions.[26] Recent evidence suggested that the design of dual JAK2/HDAC inhibitors could be a promising strategy for the treatment of leukemia, solid tumor and other related indications.[27] Both JAK2 and HDAC inhibitors demonstrated similar clinical efficacy, which have synergistic effects and can be used in combination therapy.[27] Dymock's group further confirmed that dual JAK-HDAC pathway inhibition achieved with a single molecule.[28, 29] Despite these advancements, the therapeutic value of dual JAK-HADC inhibitors remains to be further explored. Particularly, *in vivo* potency has not been achieved by the reported dual JAK2-HDAC inhibitors due to unfavorable PK properties.[28, 29]

Herein *in vivo* therapeutic values of JAK2-HADC dual inhibitors were confirmed for the first time. Novel JAK2-HADC dual inhibitors were identified, which showed excellent potency in combinational treatment of AML and resistant *Candida albicans* infections, providing a new strategy for clinical therapy of leukemia along with IFIs.

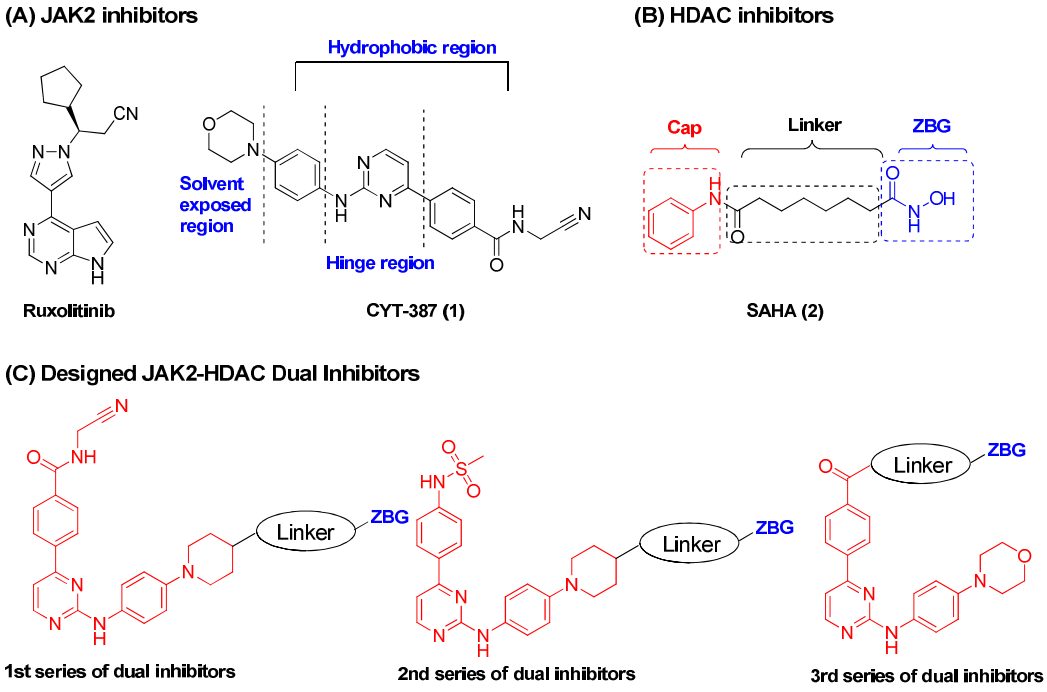

Figure 1. (**A**) Chemical structures and pharmacophore of JAK2 inhibitors; (**B**) Chemical structure and pharmacophore of HDAC inhibitors; (**C**) Design of JAK2-HDAC dual inhibitors.

RESULTS AND DISCUSSION

Structure-based Design of JAK2/HDAC Dual Inhibitors. Inspired by our previous efforts in multi-targeting drug design,[30-32] a series of novel JAK2-HADC inhibitors were designed according to synergistic effect between the two targets[27]. Generally, the pharmacophore of JAK2 inhibitors consists of a hinge region binder (typically an aminopyrimidine), two hydrophobic groups (phenyl group) and a solvent exposed part (**Figure 1A**),[33] which serves as a template in designing dual inhibitors. Since the aminopyrimidine of JAK2 inhibitor CYT-387 (**1**) has been proven to be responsible for the JAK2 inhibitory activity, the motif was maintained in designing the dual inhibitors. HDAC inhibitors (**Figure 1B**) generally consist of a hydrophobic cap

group, a linker (alkyl, alkenyl or aryl) and a zinc-binding group (ZBG, hydroxamic acid or benzamide).[34] Given that the cap group is flexible and can be replaced by other moieties to generate HDAC inhibitors, the first series of dual inhibitors (**8**, **10** and **12a-b**) were designed by merging the core group of **1** with the ZBG motif (hydroxamic acid or benzamide) through various linkers (**Figure 1C**). Moreover, on the basis of the fact that *N*-phenylmethanesulfonamide derivatives of compound **1** exhibited similar JAK2 inhibitory,[35] the second series of JAK2-HDAC inhibitors (compounds **16**, **18** and **20a-h**) were designed with the *N*-cyanomethylbenzamide/*N*-phenylmethanesulfonamide replacement. Finally, considering that a minor substitution in the hydrophobic domain of JAK2 inhibitor **1** would be tolerated, hydroxamic acid or benzamide was introduced at this position to achieve dual inhibition toward both targets (compounds **24** and **26**).

Chemistry. Chemical synthesis of JAK2-HDAC dual inhibitors are depicted in **Schemes 1-3**. Starting from 2,4-dichloropyrimidine (**3**), intermediate **7** was prepared *via* regioselective Suzuki reaction and aniline displacement reaction according to the reported methods[35] (**Scheme 1**). Treatment of compound **7** with freshly prepared hydroxylamine methanol solution gave target compound **8** or with LiOH yielded acid **9**. Condensation of **9** with *o*-phenylenediamine afforded target compound **10**, or with different amino-esters yielded esters **11a-b**, which were subsequently reacted with hydroxylamine methanol solution to give target compounds **12a-b**. Using a similar protocol, *N*-phenylmethanesulfonamide analogues (**16**, **18** and **20a-h**) were obtained according to the procedures outlined in **Scheme 2**. As shown in **Scheme 3**, target

compounds **24** and **26** were prepared using the conditions similar to those for compound **8** and **10**, respectively.

Scheme 1

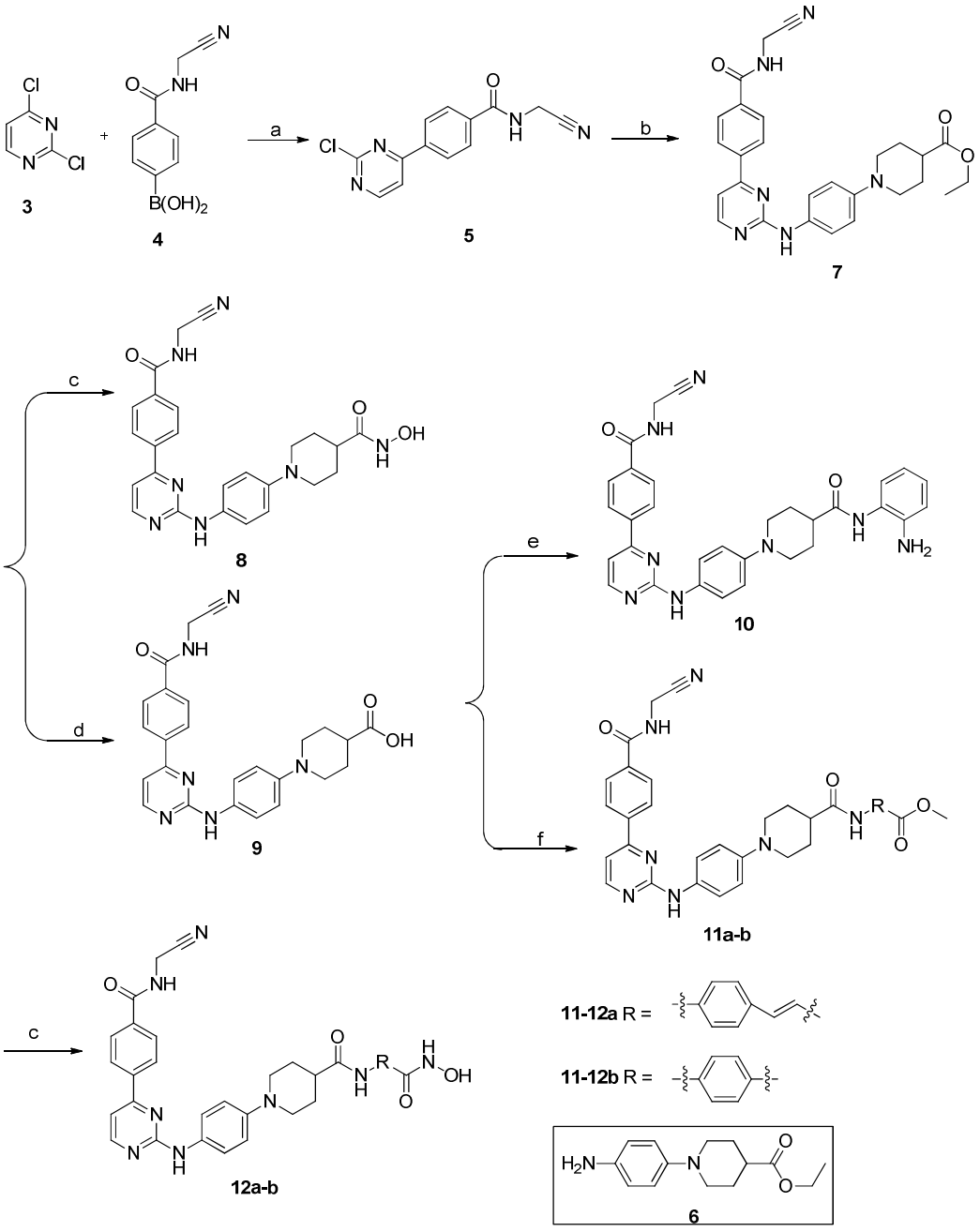

Reagents and conditions: (a) $Pd(PPh_3)_4$, toluene/*n*-PrOH, 2 M aq Na_2CO_3, 100 ^oC, 55%; (b) **6**, $TsOH \cdot H_2O$, 120 ^oC, 3 days, 82%; (c) NH_2OK, anhydrous CH_3OH, 4 h, 56%; (d) LiOH, THF/H_2O, reflux, 4 h, 85%; (e) *o*-phenylenediamine, HATU, DIPEA, DMF, rt, 4 h, 63%; (f) various amino-esters, HATU, DIPEA, DMF, rt, 4 h, 58%.

Scheme 2

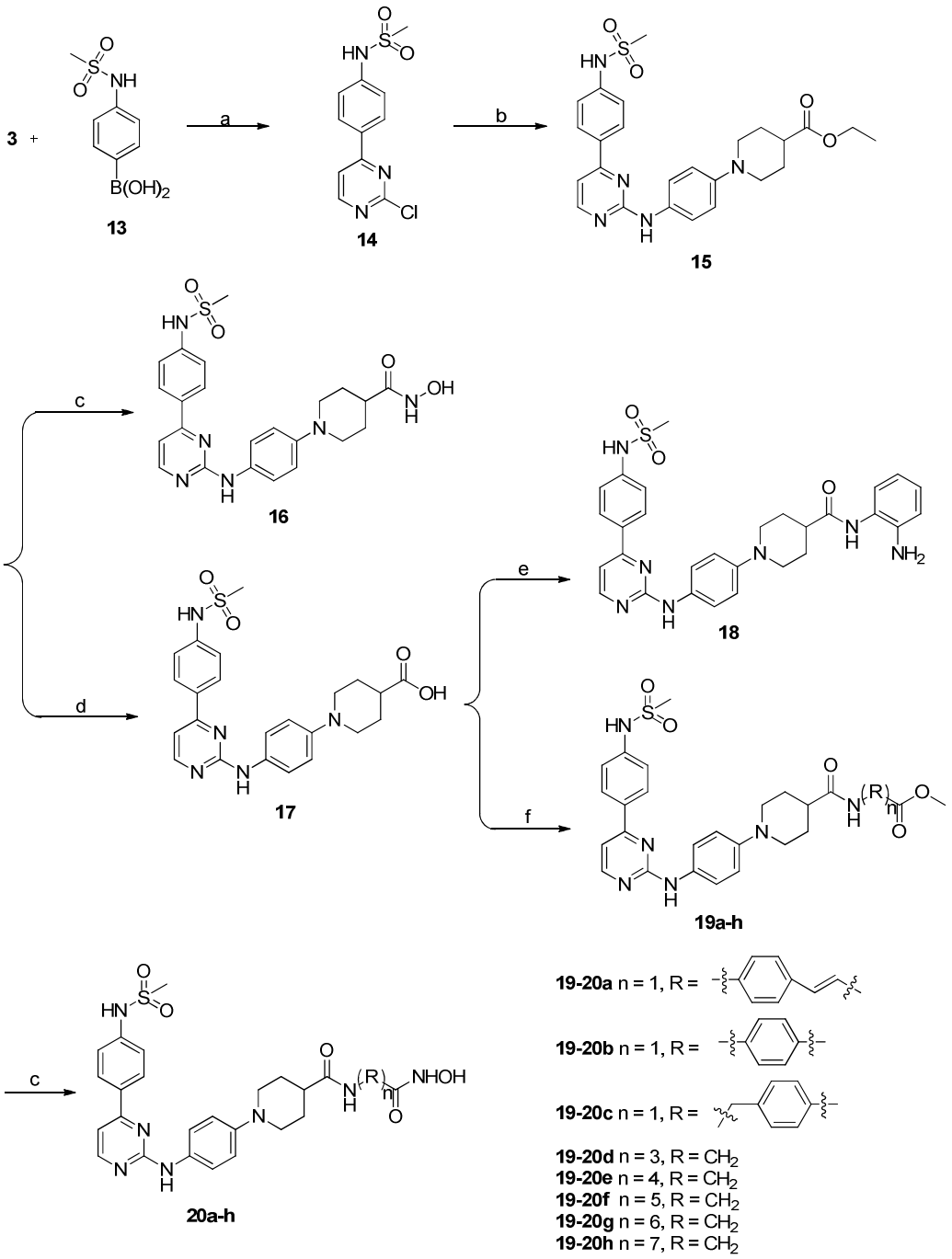

Reagents and conditions: (a) $Pd(PPh_3)_4$, toluene/*n*-PrOH, 2 M aq Na_2CO_3, 100 ^oC, 51%; (b) **6**, $TsOH \cdot H_2O$, 120 ^oC, 3 days, 77%; (c) NH_2OK, anhydrous CH_3OH, 4 h, 48%; (d) LiOH, THF/H_2O, reflux, 4 h, 82%; (e) *o*-phenylenediamine, HATU, DIPEA, DMF, rt, 4 h, 56%; (f) various amino-esters, HATU, DIPEA, DMF, rt, 4 h, 57%.

Scheme 3

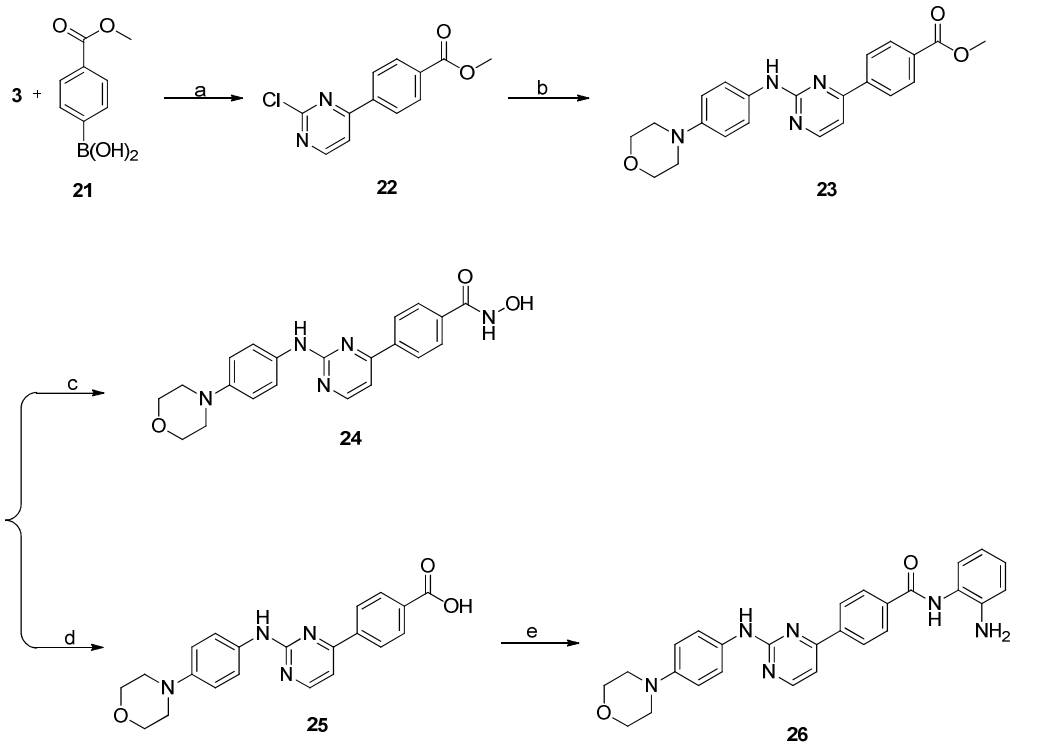

Reagents and conditions: (a) $Pd(PPh_3)_4$, toluene/*n*-PrOH, 2 M aq Na_2CO_3, 100 ^oC, 48%; (b) 4-morpholinoaniline, $TsOH \cdot H_2O$, 120 ^oC, 3 days, 73%; (c) NH_2OK, anhydrous CH_3OH, 4 h, 62%; (d) LiOH, THF/H_2O, reflux, 4 h, 86%; (e) *o*-phenylenediamine, HATU, DIPEA, DMF, rt, 4 h, 51%.

Enzyme Inhibitory Activities and *in vitro* Antitumor Potency of JAK2-HDAC Dual Inhibitors. Initially, the JAK-HDAC dual inhibitors were assayed against JAK2 and HDAC1, using compounds **1** and **2** as reference drugs. As shown in **Table 1**, the first series of dual inhibitors (compounds **8**, **10** and **12a-b**) exhibited excellent inhibitory activity against JAK2 (IC_{50} range: 4-16 nM), which were better than compound **1** (IC_{50} = 41 nM). However, their activity against HDAC1 was moderate (IC_{50} range: 1.7-23.6 μM). Then, their inhibitory activities against three human

leukemia cell-lines HL60, K562 and HEL were evaluated using the CCK-8 assay. However, only compound **10** demonstrated moderate inhibitory activity against HEL cell line (IC_{50} = 6.6 μM).

Table 1. Enzyme inhibition and *in vitro* antitumor activity of target compounds **8**, **10** and **12a-b**

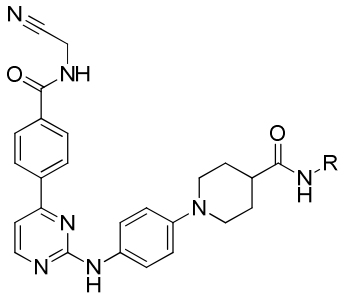

Compd.	R	IC_{50} (μM)				
		JAK2	HDAC1	HL60	K562	HEL
8		0.004 ± 0.0006	2.7 ± 0.25	> 50	> 50	> 50
10	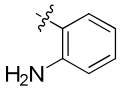	0.008 ± 0.0007	1.7 ± 0.14	> 50	>50	6.6 ± 0.65
12a	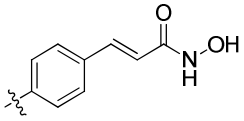	0.015 ± 0.008	5.1 ± 0.37	> 50	> 50	> 50
12b	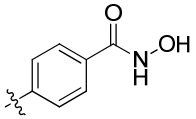	0.016 ± 0.009	24 ± 2.1	> 50	> 50	> 50
1		0.041 ± 0.005	NT[a]	8.3 ± 0.79	6.5 ± 0.58	2.3 ± 0.14
2		NT[a]	0.04 ± 0.009	1.5 ± 0.13	7.7 ± 0.64	0.86 ± 0.069
1 + **2** (1:1)		NT[a]	NT[a]	1.24 ± 0.17	1.81 ± 0.22	1.51 ± 0.26

[a]NT = not tested.

Next, the nitrile carboxamide group of the first series of compounds was replaced by *N*-phenylmethanesulfonamide. As a result, compounds **16**, **18** and **20a-c** generally displayed improved HDAC1 inhibitory activity (IC_{50} range: 0.25-2.9 μM), while excellent JAK2 inhibitory activity was retained. More importantly, their antitumor activities were also increased. For the ZBG, hydroxamic acid derivative **20a** showed better antitumor activity than benzamide derivative **18**. Thus, more derivatives containing various alkyl linkers were investigated (compounds **20d-h**). Enzyme assays showed that their JAK2 and HDAC1 inhibitory activities were further improved (JAK2 IC_{50} range: 1-3 nM; HDAC1 IC_{50} range: 0.018-9 μM). SAR studies indicated that the HDAC1 inhibitory activity increased along with the elongation of the linker (**20h** > **20g** > **20f** > **20e** > **20d**). Among the second series of dual inhibitors, compound **20a** exhibited the best inhibitory activity against HEL cells (IC_{50} = 0.34 μM), which was more potent than JAK2 inhibitor **1** (IC_{50} = 2.3 μM) and HDAC inhibitor **2** (IC_{50} = 0.86 μM), although its JAK2 and HDAC inhibition activities were less potent than the two inhibitors. The combination of **1** and **2** were also evaluated to investigate the synergic effect between JAK and HDAC inhibitors. Compounds **1** and **2** (1:1) showed improved antitumor potency than **1** and **2** dosed alone against HL60 and K562 cells. Thus, JAK and HDAC inhibitors showed synergic effect in cancer cells. Moreover, compound **20a** showed better HEL inhibitory activities than the combination of **1** and **2** (IC_{50} = 1.51 μM). These results indicated that the cytotoxicity might be the consequence of the synergism of the JAK2 and HDAC inhibition.

Table 2. Enzyme inhibition and *in vitro* antitumor activity of target compounds **16**, **18** and **20a-h**

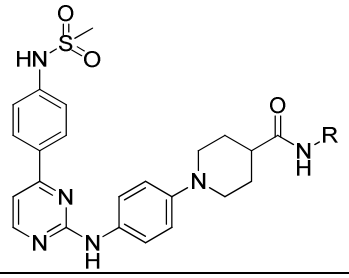

Compd.	R	IC_{50} (μM)				
		JAK2	HDAC1	HL60	K562	HEL
16		0.001 ± 0.0003	2.9 ± 0.15	> 50	18 ± 1.8	> 50
18	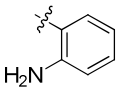	0.002 ± 0.0004	2.1 ± 0.12	16 ± 2.3	9.5 ± 0.86	3.2 ± 0.25
20a	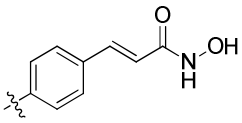	0.008 ± 0.0007	0.25 ± 0.025	1.5 ± 0.12	8.7 ± 0.71	0.34 ± 0.025
20b	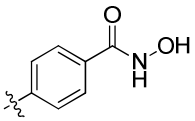	0.002 ± 0.0003	0.38 ± 0.06	11 ± 1.2	8.6 ± 0.72	2.0 ± 0.16
20c	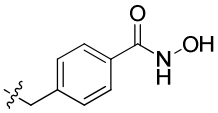	0.018 ± 0.0007	1.1 ± 0.16	> 50	10 ± 2.2	6.3 ± 0.58
20d	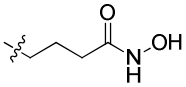	0.001 ± 0.0004	9.2 ± 0.78	> 50	12 ± 2.1	12 ± 2.6
20e	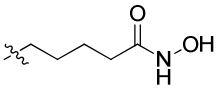	0.001 ±0.0002	2.2 ± 0.18	> 50	11 ± 1.8	8.1 ± 0.76
20f	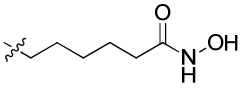	0.003 ± 0.0006	0.35 ± 0.026	37 ± 3.5	10 ± 1.3	17 ± 1.6
20g	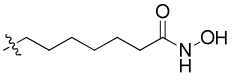	0.002 ± 0.0004	0.25 ± 0.021	12 ± 1.3	8.9 ± 0.78	3.9 ± 0.25
20h	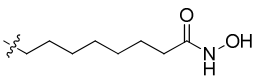	0.002 ± 0.0003	0.018 ± 0.006	> 50	5.9 ± 0.48	1.8 ± 0.12

1	-	0.041 ± 0.005	NT[a]	8.3 ± 0.79	6.5 ± 0.58	2.3 ± 0.14
2	-	NT[a]	0.04 ± 0.009	1.5 ± 0.13	7.7 ± 0.64	0.86 ± 0.069
1 + **2** (1:1)		NT[a]	NT[a]	1.24 ± 0.17	1.81 ± 0.22	1.51 ± 0.26

[a]NT = not tested.

Finally, ZBGs (hydroxamic acid or benzamide) were used to replace the *N*-cyanomethylbenzamide group in JAK2 inhibitor **1** (compounds **24** and **26**). As listed in **Table 3**, the ZBGs were important for the inhibition of enzyme and leukemia cell lines. Compound **24** containing hydroxamic acid as the ZBG displayed good inhibitory activity toward HDAC1 (IC_{50} = 0.16 μM) and JAK2 (IC_{50} = 0.085 μM), and the antitumor activities were comparable to lead compounds **1** and **2**. In contrast, benzamide derivative **26** only exhibited moderate JAK2 inhibitory activity (IC_{50} = 0.11 μM), and was totally inactive in inhibiting HDAC1 and cell proliferation.

Table 3. Enzyme inhibition and *in vitro* antitumor activity of the target compounds **24** and **26**

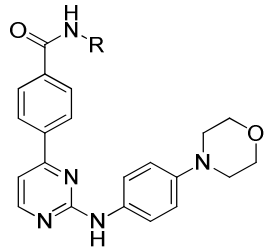

Compd.	R	IC_{50} (μM)				
		JAK2	HDAC1	HL60	K562	HEL
24		0.085 ± 0.006	0.16 ± 0.03	6.1 ± 0.36	4.0 ± 0.32	3.5 ± 0.26
26	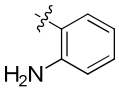	0.11 ± 0.02	> 50	> 50	> 50	> 50
1	-	0.041 ± 0.005	NT[a]	8.3 ± 0.79	6.5 ± 0.58	2.3 ± 0.14
2	-	NT[a]	0.04 ±0.009	1.5 ± 0.13	7.7 ± 0.64	0.86 ± 0.069
1 + **2** (1:1)		NT[a]	NT[a]	1.24 ± 0.17	1.81 ± 0.22	1.51 ± 0.26

[a]NT = not tested.

JAK2/HDAC1 Dual Inhibitors Showed Excellent Synergistic Effect with FLC against Resistant *C. albicans* Isolates. HDACs are important regulators of heat shock protein 90 (Hsp90), which is essential for fungal survival and is associated with antifungal drug resistance.[36] HDAC inhibitors were reported to enhance the potency of antifungal agents (*e.g.* azoles and echinocandins) against various fungal pathogens including resistant isolates.[37-39] Thus, the antifungal activity and synergistic effects of JAK2/HDAC dual inhibitors were evaluated against FLC-resistant *C. albicans* isolates 0304103, 100 and 071922. The antifungal activity was expressed as the

minimum inhibitory concentration that achieves 50% of inhibition (MIC_{50}) using the checkerboard microdilution assay according to the methods of the CLSI (formerly NCCLS)(M27-A).[40] The synergistic effects were evaluated by the fractional inhibitory concentration (FIC) index and the synergism was defined by FIC index of ≤ 0.5.[41] As shown in **Table 4**, most of the target compounds were inactive to three FLC-resistant *C. albicans* isolates when used alone ($MIC_{50} > 64$ μg/mL). Only compounds **20d-f** showed moderate antifungal activity against FLC-resistant *C. albicans* 0304103 ($MIC_{50} = 32$ μg/mL). When used in combination with FLC, a majority of compounds (**8**, **12a**, **16**, **20a**, **20c-h** and **24**) exhibited excellent synergistic effects against FLC-resistant *C. albicans* strain 0304103 with the FIC index ranging from 0.078 to 0.50. SAR studies indicated that compounds containing the benzamide ZBG (*e.g.* compounds **10**, **18** and **26**) were devoid of the synergistic antifungal effects. HDAC inhibitor **2** and the combination of **1** and **2** also showed synergistic effects against *C. albicans* 0304103 strain, whereas the synergism was lost for strains 100 and 0710922. In contrast, obvious synergistic effect (FIC range: 0.039 to 0.5) was retained for dual inhibitors **8**, **16**, **20a**, **20c-e**, **20g-h** and **24** against these resistant strains. Compounds **12a**, **20a**, **20g-h** and **24** exhibited good synergism (FIC index range: 0.14 to 0.5). Considering the potent antitumor activity and promising antifungal profile of compounds **20a**, **20h** and **24**, they were subjected for further evaluations.

Table 4. Antifungal activity and synergistic effects of target compounds with FLC against resistant *C. albicans* isolates by the microdilution assay

Strains	0304103 (MIC_{50}, μg/mL)					100 (MIC_{50}, μg/mL)					0710922 (MIC_{50}, μg/mL)				
	used alone		used in combination		FIC Index[a]	used alone		used in combination		FIC Index	used alone		used in combination		FIC Index
	FLC	Cmpd.	FLC	Cmpd.		FLC	Cmpd.	FLC	Cmpd.		FLC	Cmpd.	FLC	Cmpd.	
8	> 64	> 64	0.25	8	0.13	> 64	> 64	0.5	2	0.039	> 64	> 64	1	64	1.02
10	> 64	> 64	> 64	> 64	> 2	> 64	> 64	> 64	> 64	> 2	> 64	> 64	64	64	2
12a	> 64	> 64	1	4	0.078	> 64	> 64	1	64	1.02	> 64	> 64	2	16	0.31
12b	> 64	> 64	0.5	64	1.01	> 64	> 64	2	64	1.03	> 64	> 64	> 64	> 64	> 2
16	> 64	> 64	0.5	4	0.07	> 64	> 64	1	8	0.14	> 64	> 64	0.25	32	0.51
18	> 64	> 64	> 64	> 64	> 2	> 64	> 64	64	64	2	> 64	> 64	> 64	> 64	> 2
20a	> 64	> 64	0.5	4	0.07	> 64	> 64	0.5	4	0.07	> 64	> 64	1	8	0.14
20b	> 64	> 64	> 64	> 64	> 2	> 64	> 64	16	64	1.25	> 64	> 64	> 64	> 64	> 2
20c	> 64	> 64	2	8	0.15	> 64	> 64	1	4	0.078	> 64	> 64	0.5	64	1.01
20d	> 64	32	4	8	0.31	> 64	> 64	1	8	0.14	> 64	> 64	0.5	32	0.51

20e	> 64	32	0.5	16	0.50	> 64	> 64	0.5	16	0.26	> 64	> 64	0.5	32	0.51
20f	> 64	32	0.5	16	0.50	> 64	32	0.25	16	0.50	> 64	> 64	64	64	2
20g	> 64	> 64	0.5	8	0.13	> 64	> 64	0.25	8	0.13	> 64	> 64	0.25	32	0.50
20h	> 64	> 64	0.25	8	0.13	> 64	> 64	0.5	8	0.13	> 64	> 64	0.25	16	0.26
24	> 64	> 64	0.5	4	0.07	> 64	> 64	0.5	8	0.13	> 64	> 64	1	16	0.27
26	> 64	> 64	> 64	> 64	> 2	> 64	> 64	0.5	64	1.01	> 64	> 64	> 64	> 64	> 2
1	> 64	> 64	> 64	> 64	> 2	> 64	> 64	> 64	> 64	> 2	> 64	> 64	64	64	2
2	> 64	> 64	0.25	16	0.25	> 64	> 64	0.5	32	0.51	> 64	> 64	1	64	1.02
1 + 2 (1:1)	> 64	> 64	0.5	16	0.26	> 64	> 64	1	64	1.01	> 64	> 64	4	64	1.06

[a] FIC index is defined as the sum of MIC of each drug used in combination divided by the MIC of the drug used alone. Synergy and antagonism were defined by FIC index of ≤ 0.5 and > 4, respectively. An FIC index between 0.5 and 4 was considered indifferent.

Binding Mode of the JAK2-HDAC Dual Inhibitors. To investigate the binding mode of compounds **20a**, **20h** and **24** with JAK2 and HDAC1, molecular docking studies were performed. Compound **20a** bound with HDAC1 (PDB ID: 4BKX[42]) mainly through the linker and ZBG (**Figure 2A**). The hydroxamic acid of **20a** coordinated to the catalytic Zn^{2+} of HDAC1 and formed two hydrogen bonds with Gly146 and His178, respectively. The hydrophobic cinnamamide group formed π-π stacking interactions with His178, Phe150 and Phe205. Moreover, the *N*-phenylmethanesulfonamide moiety formed three additional hydrogen bonds with Glu146, Lys143 and Ser148. Similarly, the ZBG of compound **20h** was engaged with a hydrogen boding network with Gly138, Asp176 and Tyr303 (**Figure 2B**). The *N*-phenylmethanesulfonamide group interacted with Glu146 through a hydrogen bond. For compound **24**, the hydroxamic acid moiety formed coordination interaction and a hydrogen bond with Zn^{2+} and Gly149, respectively (**Figure 2C**). In addition, its aromatic linker and phenyl group in the cap formed π-π stacking interactions with Phe205. In contrast, the terminal *N*-(2-aminophenyl)benzamide of compound **26** forced the whole molecule located at the outside of the active site, which might be the reason why **26** was totally inactive toward HDAC1 (**Figure S1** in **Supporting Information**).

In JAK2 (PDB ID: 4AQC[43]), the aminopyrimidine scaffold of compound **20a** formed hydrogen bonds to the backbone of Leu932 in the hinge region (**Figure 2D**). Its *N*-phenylmethanesulfonamide group formed an additional hydrogen bond with Asp994. Moreover, the linker and ZBG extended out of the binding site and formed

hydrogen bonds with Asp939 and Arg980, respectively. As shown in **Figure 3E-F**, the binding modes of compounds **20h** and **24** with JAK2 were similar to that of **20a** where hydrogen bonds between animopyrimidine and the backbone of Leu932 were observed. The *N*-phenylmethanesulfonamide and hydroxamic acid moiety of compound **20h** formed hydrogen bonds with Asp994 and Lys857, respectively. Moreover, an additional hydrogen bond was found between the hydroxamic acid group of compound **24** and Asn981.

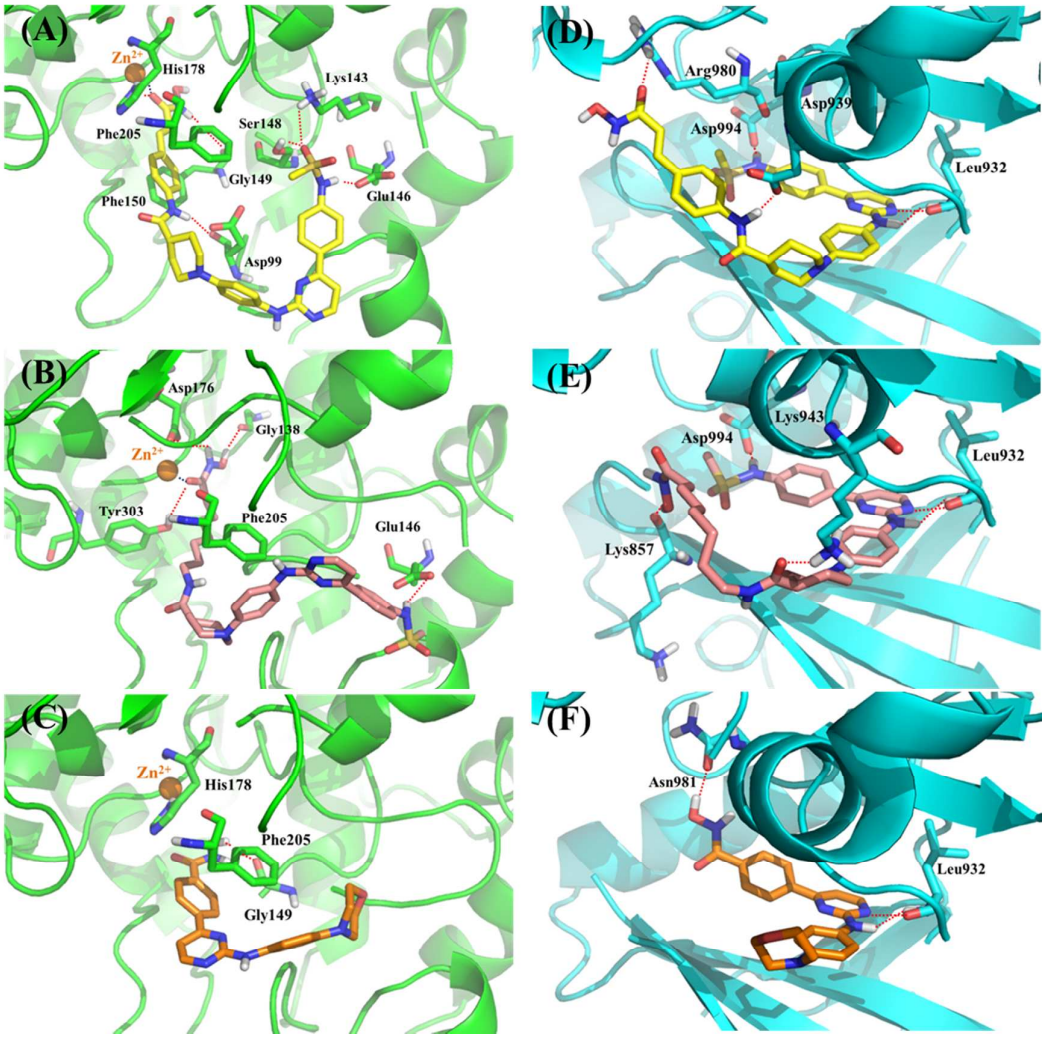

Figure 2. Proposed binding mode of compounds **20a**, **20h** and **24** in the active site of HDAC1 (PDB ID: 4BKX, **A-C**) and in the ATP-binding site of JAK2 (PDB ID:

4AQC, **D-F**). The carbons of **20a**, **20h** and **24** are colored in yellow, pink and orange, respectively. Oxygen atoms are colored in red and nitrogen atoms in blue. Hydrogen bonds are indicated with dashed lines. The figure was generated using PyMol (http://www.pymol.org/).

***In vitro* JAK and HDAC Isoform Selectivity of Compounds 20a, 20h and 24.** To obtain evidence for the JAK and HDAC isoform selectivity, compounds **20a**, **20h** and **24** were evaluated against four JAK isoforms (JAK1, JAK2, JAK3, TYK2) and five HDAC isoforms (HDAC1, HDAC2, HDAC3, HDAC6 and HDAC8). As depicted in **Table 5**, three compounds exhibited remarkable selectivity for JAK2 over other isoforms. For HDACs, surprisingly, three compounds displayed different selective profiles (**Table 6**, **Table S1** and **Table S2** in **Supporting Information**). Compound **20a** showed good selectivity for HDAC6 (IC_{50} = 46 nM), whereas compound **24** was observed to be a HDAC3 selective inhibitor (IC_{50} = 45 nM). In contrast, compound **20h** showed similar inhibitory activity for HDAC1 and HDAC3 with an IC_{50} value of 18 nM and 17 nM, respectively.

Table 5. JAK isoform profiling of compounds **20a**, **20h** and **24**

	IC_{50} (nM)		
	20a	**20h**	**24**
JAK1	359 ± 22	76 ± 3.5	69 ± 4.1
JAK2	8.4 ± 0.7	2.2 ± 0.3	85 ± 6.0
JAK3	121 ± 13	144 ± 14	517 ± 27
TYK2	46 ± 1.7	74 ± 6.4	419 ± 71

Table 6. HDAC isoform profiling of compounds **20a**, **20h** and **24**

	IC_{50} (nM)

	20a	20h	24
HDAC1	1100 ± 140	18 ± 6.0	160 ± 32
HDAC2	7472 ± 856	132 ± 28	1704 ± 115
HDAC3	234 ± 31	17 ± 1.2	45 ± 3.3
HDAC6	46 ± 1.7	74 ± 6.4	419 ± 71
HDAC8	6065 ± 529	572 ± 49	609 ± 85

Due to HDAC selective profile of compounds **20a** and **24**, selective HDAC6 inhibitors Tubastatin A (**27**)[44] and ACY1215 (**28**)[45] and selective HDAC3 inhibitor RGFP966 (**29**)[46] were further assayed (chemical structures see **Figure S4** in **Supporting Information**). As listed in **Table S3**, HDAC6 inhibitors **27** and **28** exhibited moderate inhibitory activities against HL60, K562 and HEL cell lines (IC_{50} range: 3.75-23.88 μM), which were less active than compound **20a**. For HDAC3 inhibitor **29**, it only showed marginal activity (IC_{50} range: 21.71-33.58 μM). The combinations of JAK2 inhibitor **1** with three selected HDAC inhibitors were also investigated for antiproliferative activities. When compound **1** was used in combination with HDAC6 inhibitor **27** or **28**, the inhibitory activities were not significantly changed (IC_{50} range: 2.54-8.55 μM), indicating that there was no synergistic effect between them. In contrast, when compound **1** was used in combination with HDAC3 inhibitor **29**, improved antitumor activity was observed (IC_{50} range: 1.64-4.19 μM). For the antifungal activity, compounds **27-29** were inactive to three FLC-resistant *C. albicans* isolates (MIC_{50} > 64 μg/mL). When used in combination, only compound **28** showed synergistic effects with FLC against *C. albicans* 0304103 strain (**Table S4** in **Supporting Information**).

Compounds 20a, 20h and 24 Induced Apoptosis and Cell Cycle Arrest. To investigate the effect of the selected dual inhibitors on the induction of apoptosis, compounds **20a**, **20h** and **24** were evaluated by annexin VFTIC/propidium iodide (PI) assay. HEL cells were incubated with vehicle alone or tested compounds at 5 μM and 10 μM for 48 h. As shown in **Figure 3**, compounds **20a**, **20h** and **24** caused a dose-dependent induction of apoptosis in HEL cells. The percentages of apoptotic cells for compounds **20a**, **20h** and **24** at the concentration of 10 μM were 70.62%, 89.2% and 86.2%, respectively, which were significantly higher than JAK2 inhibitor **1** (25.9% apoptotic cells at 10 μM, $P < 0.001$).

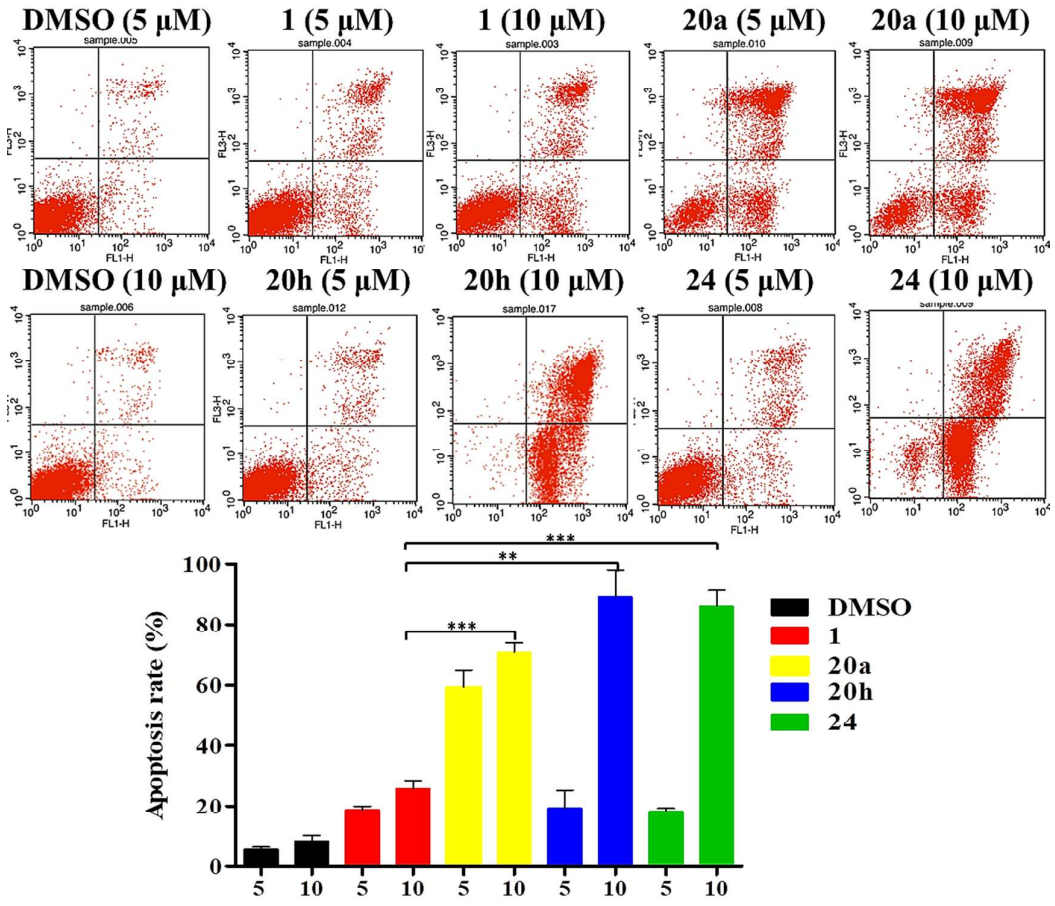

Figure 3. Cell apoptosis induced by compounds **20a**, **20h** and **24**. HEL cells were incubated with the indicated concentrations of **1**, **20a**, **20h** and **24** for 48 h. Cells treated with DMSO were used for comparison. Data were represented as mean ± standard deviation from three independent experiments. * $P < 0.05$, ** $P < 0.01$, *** $P < 0.001$, determined with Student's *t* test.

To probe the effect of compounds **20a**, **20h** and **24** on various phases of cell cycle progression, flow cytometry method was performed. HEL cells were treated with vehicle alone or compound **20a**, **20h** and **24** at different concentrations (**Figure 4**). After treating with compound **20a** at 1 μM and 5 μM for 48 h, the ratios in G_2/M phase of cell cycle were 11.75% and 28.14%, respectively. While the ratios of cells untreated in G_2/M phase of the cell cycle were 9.32% and 9.31%, respectively. Interestingly, the ratios of cells incubated with compound **20h** at 1 μM and 5 μM in G_2/M phase of cell cycle were not dramatically changed (8.23% and 8.12%, respectively), but the ratios in S phase of cell cycle were 25.56% and 34.37%, respectively. Similarly, the ratios of cells treated with compound **24** at 5 μM and 10 μM in the S phase of the cell cycle were 18.90% and 48.68%, respectively. Taken together, compounds **20a** arrested HEL cells mainly at the G_2/M phase ($P < 0.001$), and compounds **20h** and **24** could significantly arrest HEL cells at the S phase ($P < 0.001$).

Compound **2** arrested HEL cells mainly in G_1 phase,[47] while JAK2 inhibitors induced cell cycle arrest at the G_2/M phase in HEL cells.[48] HDAC6 selective inhibitors (**27** and **28**) and HDAC3 selective inhibitor **29** were further evaluated on

the various phases of cell cycle progression (**Figure S5** in **Supporting Information**). Surprisingly, all the three compounds arrested HEL cells at G_1 phase ($P < 0.05$), which was different with compounds **20a**, **20h** and **24**. These data suggest that compound **20a** arrested HEL cells at G_2/M phase possibly because of the inhibition of JAK2. The underlying mechanisms why compounds **20h** and **24** arrested HEL cells at S phase remained to be further investigated.

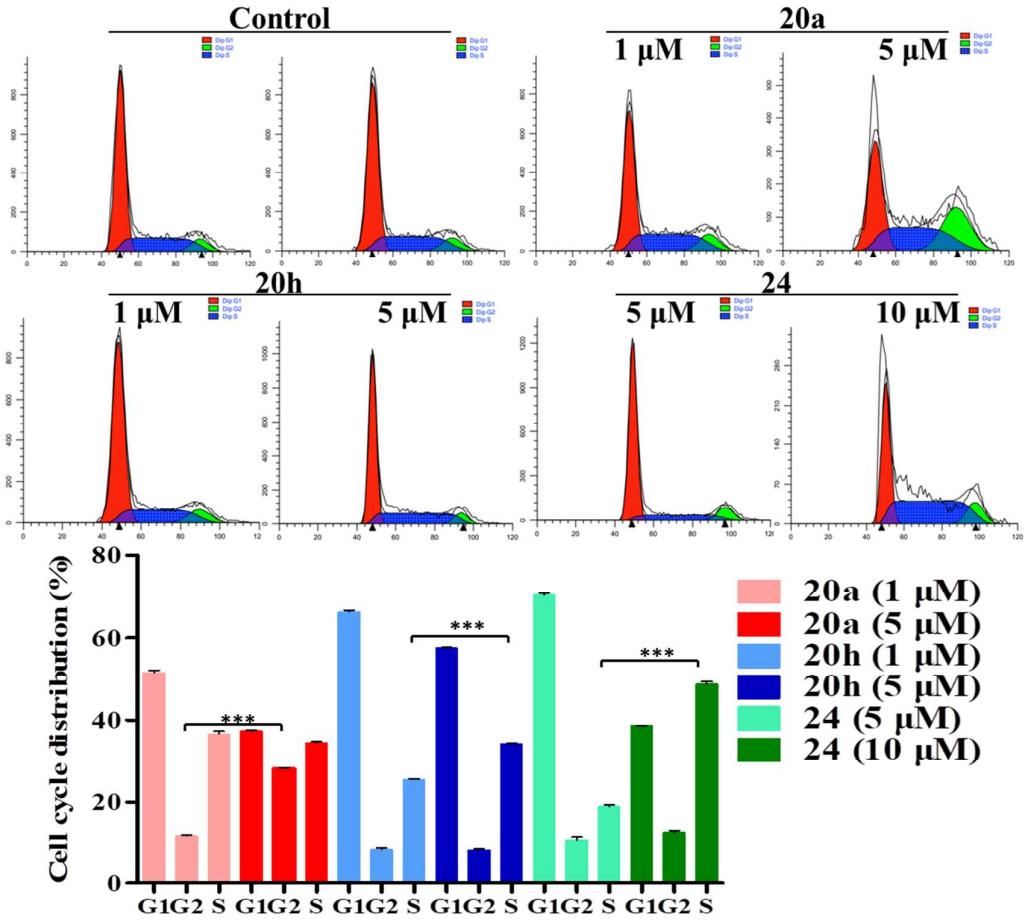

Figure 4. Cell cycle analysis after 48 h of treatment. HEL cells treated with **20a**, **20h** and **24** at different concentrations for 48 h were assayed by flow cytometry after staining with PI. Data were represented as mean ± standard deviation from three independent experiments. * $P < 0.05$, ** $P < 0.01$, *** $P < 0.001$, determined with Student's *t* test.

Compounds 20a, 20h and 24 Inhibited JAK and HDAC in HEL Cells. To determine whether the three selected compounds inhibited both the JAK-STAT and HDAC pathway in cells, western blot assay was performed to evaluate the effect of compounds **20a**, **20h** and **24** on the acetylation level of histone 3, histone 4 and phosphorylation of STAT5. HEL cells were exposed to them at 0.2 μM, 1 μM and 5 μM for 24 h. As shown in **Figure 5**, all the three compounds caused a dramatic increase in acetyl-histone 3 and acetyl-histone 4 in a dose dependent manner. On the other hand, exposure of HEL cells to compounds **20a**, **20h** and **24** resulted in dose-dependent decreases in STAT5 phosphorylation. Taken together, the results clearly confirmed that the designed JAK2/HDAC inhibitors inhibited both targets in HEL cells.

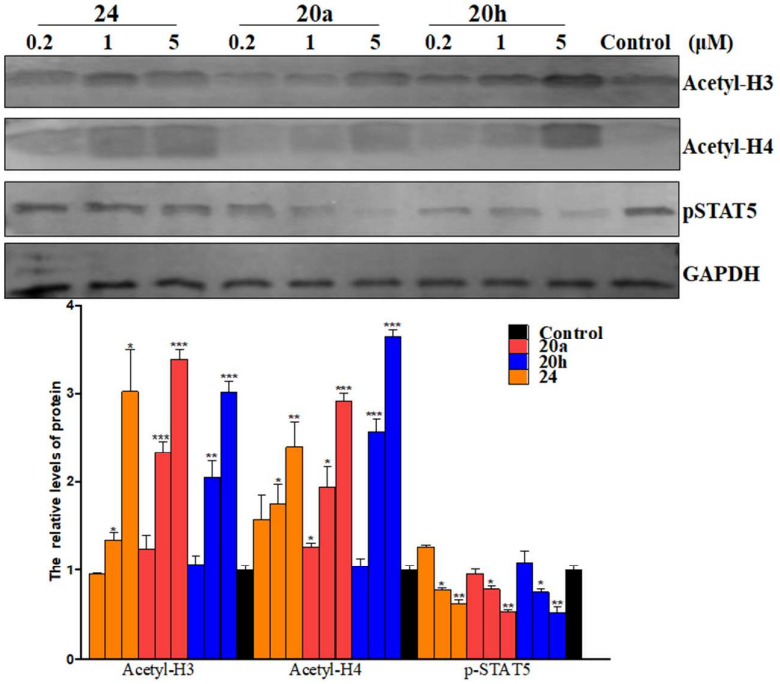

Figure 5. Effects of compounds **20a**, **20h** and **24** on the levels of acetyl-H3, acetyl-H4 and STAT5 phosphorylation in HEL cells. * $P < 0.05$, ** $P < 0.01$, *** $P < 0.001$ versus the control group.

Synergistic Dose-response Relationships against FLC-resistant *C. albicans* cells. The synergistic dose-response relationship of compounds **20a**, **20h** and **24** against FLC-resistant *C. albicans* strain 0304103 was further investigated. The cells were treated with different concentrations of FLC (1 μg/mL to 32 μg/mL) and compounds **20a**, **20h** and **24** (2 μg/mL to 32 μg/mL) using the growth curves assay (**Figure 6**). High dosage of target compounds (32 μg/mL) or 1 μg/mL of FLC alone exhibited no antifungal effect, but the antifungal effect was significantly improved when they were used together (**Figure 6A-C**). Interestingly, the results also indicated that the synergistic effect mainly depended on the concentration of the dual inhibitors instead of FLC (Figure **6D-F**).

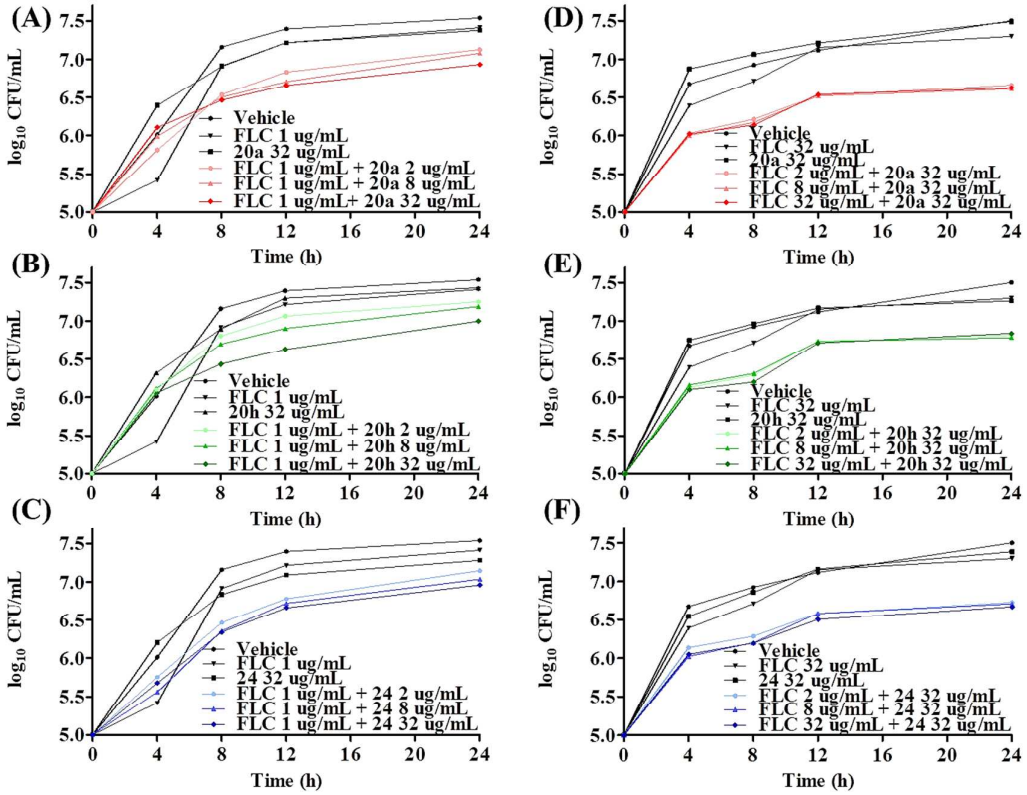

Figure 6. Synergistic dose-response relationships of the drug combination. Growth curves of *C. albicans* 0304103 cells incubated with 1 μg/mL of FLC and different

concentration of compounds **20a** (**A**), **20h** (**B**) and **24** (**C**) for 24 h. Growth curves of *C. albicans* 0304103 cells treated with 32 μg/mL of compounds **20a** (**D**), **20h** (**E**) and **24** (**F**) and different concentration of FLC for 24 h.

Compounds 20a and 24 Inhibited the Biofilm Formation of FLC-resistant *C. albicans* Cells. *C. albicans* biofilms are complex communities that form on tissues and implanted medical devices, causing drug resistance and repeated infections in clinics.[49, 50] The effect of compounds **20a**, **20h** and **24** on FLC-resistant *C. albicans* (strain number: 0304103) biofilm formation was evaluated by the XTT reduction assay.[51, 52] 1×10^6 cells of FLC-resistant *C. albicans* strain and 64 μg/mL of FLC were incubated in 96-well plate for 90 min, and then treated with different concentrations of compounds **20a**, **20h** and **24** for 24 h. An equivalent volume of DMSO was added as the control. Interestingly, they inhibited the biofilm formation in a dose-dependent manner (**Figure 8**). More specifically, 16 μg/mL of compound **20a** or **24** inhibited biofilm formation by about 30% ($P < 0.05$), and the anti-biofilm effect increased with the increasing of the concentration. However, compound **20h** was less active.

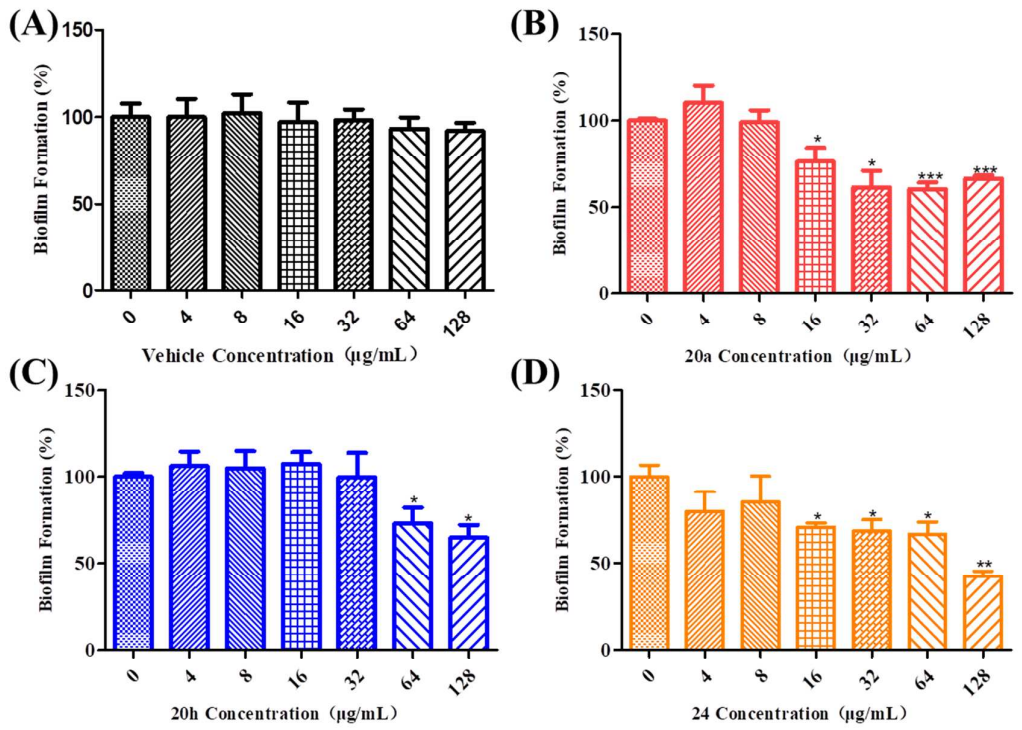

Figure 7. Inhibition of FLC-resistant *C. albicans* biofilm formation by DMSO (**A**) compounds **20a** (**B**), **20h** (**C**) and **24** (**D**) using the XTT reduction assay. The results were presented as a percentage compared to the control biofilms formed without compound treatment. * $P < 0.05$, ** $P < 0.01$, *** $P < 0.001$ versus the control group.

Compounds 20a, 20h and 24 Showed Potent *in vivo* Antitumor Activity in AML Xenograft Models. To investigate the *in vivo* antitumor effect, xenograft models of AML were prepared. First, compounds **20a**, **20h** and **24** were tested in the HEL xenograft model. HEL cells (5×10^6) were subcutaneously implanted in the right flanks of the female nude mice. When implanted tumor reached a volume of 100-300 mm^3, compounds **20a**, **20h** and **24** were administered intraperitoneally (*i.p*) at 10 mg/kg twice a day for 21 consecutive days. Compounds **1** and **2** were used as the positive controls. As shown in **Figure 8A** and **8B**, treatment with three compounds

caused significantly reduction in tumor growth. Moreover, all of them were observed to be well tolerated during the test and no significant loss of body weight was observed (**Figure S2** in **Supporting Information**), indicating that their toxicity is low. Particularly, compound **24** revealed the best *in vivo* antitumor activity, which showed higher TGI value (59.9%) and lower T/C value (41.1%) than positive drugs **1** (TGI = 40.2%; T/C = 68.3%) and **2** (TGI = 13.8%; T/C = 87.9%). In contrast, selective HDAC6 inhibitors (**27** and **28**) and selective HDAC3 inhibitor **29** only exhibited weak antitumor activity in the xenograft HEL model with a TGI value of 18.8%, 14.1% and 16.4, respectively (**Figure S6** in Supporting Information).

Furthermore, the three compounds were evaluated on HEL AML xenograft model. HEL cells (5×10^6) were injected *via* tail vein to sublethally irradiated female 5-week SCID mice. At the dose of 10 mg/kg (once daily), compounds **20a**, **20h** and **24** resulted in a significant increase in the survival rate (**Figure 8C**). More specifically, after about 10 days, mice in vehicle group, positive drug **1**- or **2**-treated group died off sharply. In contrast, the lifetime of mice lasted as long as 27 days when treated with compounds **20h** and **24**. On the day 32, the survival percentage in **20a**-treated group was 37.5%. Kaplan-Meier analysis indicated that the three tested compounds significantly extended the lifetime and survival of leukemic mice. Three mice were picked from each group and sacrificed for histological analysis. Meanwhile, spleens in leukemic mice were dissected and weighted (**Figure 8D** and **Figure S3** in **Supporting Information**). Enlarged spleens were found notably in vehicle-treated mice, which could be alleviated when treated with compounds **20a**, **20h** and **24**. This

can be regarded as positive effect in AML therapies, because enlarged spleens are usually considered as a symbol of pathological tissue infiltration.[53, 54]. In contrast, positive drugs **1** and **2** showed no effect in the reduction of spleen enlargement. Similarly, selective HDAC6 (**27** and **28**) and HDAC3 (**29**) inhibitors also could not extend the lifetime of leukemic mice ($P > 0.05$) and reduce the enlargement of spleen ($P > 0.05$).

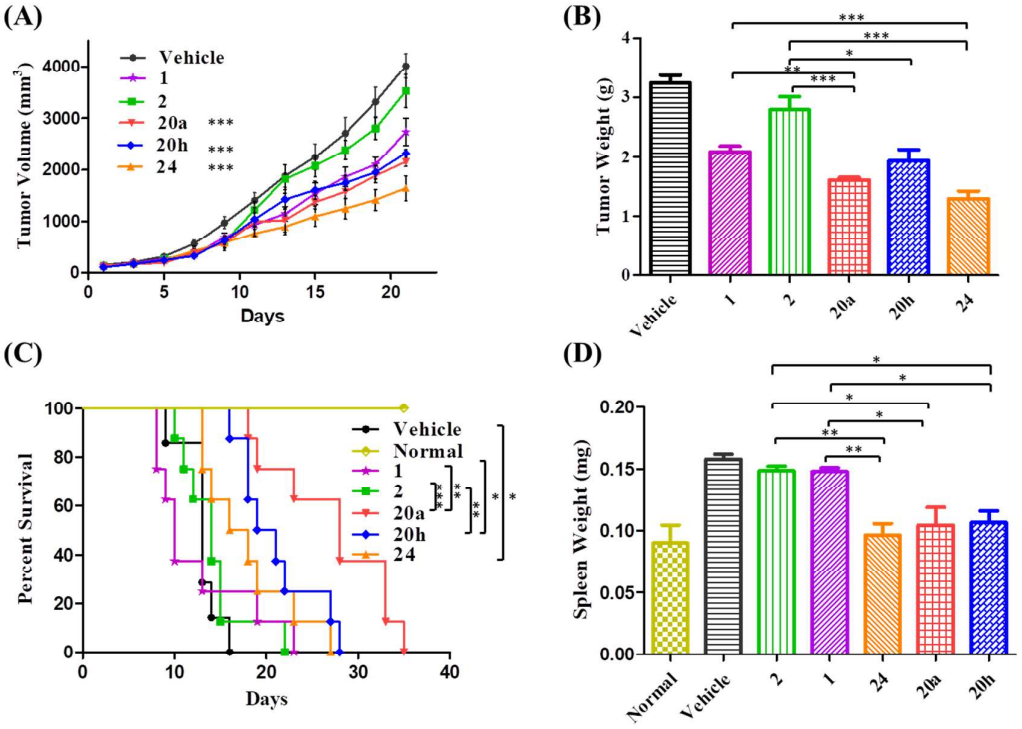

Figure 8. Compounds **20a**, **20h** and **24** suppress tumor growth and improve survival of leukemic mice *in vivo*. (**A**) The efficacy of compounds **20a**, **20h** and **24** in the HEL xenogarft model. Data were represented as mean ± standard deviation. * $P < 0.05$, ** $P < 0.01$, *** $P < 0.001$ versus the control group, determined with Student's *t* test. (**B**) Tumor weight of dissected HEL tumor tissues. (**C**) The Kaplan-Meier curves of leukemic mice in control (vehicle), **1**, **2**, **20a**, **20h** and **24** treatment groups. * $P < 0.05$, ** $P < 0.01$, *** $P < 0.001$ by log-rank test for significance. (**D**) The spleen weight of

the killed leukemic mice. * $P < 0.05$, ** $P < 0.01$, determined with Student's *t* test.

Compounds 20a, 20h and 24 Effectively Synergized with FLC to Treat Resistant *C. albicans* Infections in Disseminated Candidiasis Models. Given the potent synergistic effects between FLC and compounds **20a**, **20h** and **24**, their therapeutic efficacy in resistant *C. albicans* models were investigated. Immunocompromised ICR mice were injected *via* tail vein with 15×10^4 cells of FLC-resistant *C. albicans* (strain number: 0304103) and were treated daily with vehicle, compounds **20a**, **20h** and **24** (5 mg/kg), FLC (1 mg/kg), or the drug combinations (**Figure 9**). The median survival time (MST) of the vehicle mice was 4.5 days and FLC-treated group only resulted in minor increase of survival time (MST = 7.5 days). In combination therapy groups, the MST of FLC/**1** combination and FLC/**2** combination treated group is 5.5 days and 10 days, respectively. In contrast, the MST of mice treated with combination of FLC and compounds **20a**, **20h** and **24** were significantly increased (MST = 11.5 days, 13 days and 11 days, respectively). When used alone, selective HDAC6 (**27** and **28**) and HDAC3 (**29**) inhibitors had no effect on the extension of mice survival time (**Figure S7** in **Supporting Information**). In combination therapy groups, the MST of FLC/**27** combination, FLC/**28** combination and FLC/**29** combination treated group is 4.5 days, 5 days and 5 days, respectively. These results indicated three selective HDAC inhibitors had no therapeutic effect on IFI mice (**Figure S6** in **Supporting Information**). The results highlighted the advantages of JAK2/HDAC dual inhibitors in combinational treatment of resistant *C. albicans* infections.

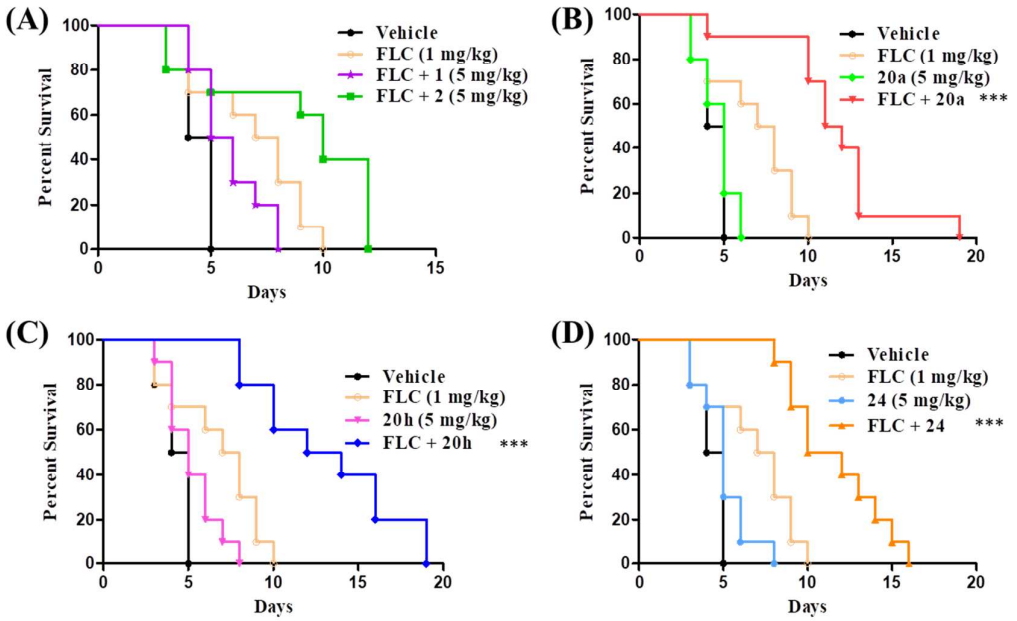

Figure 9. The therapeutic efficacy of compounds and FLC in FLC-resistant *C. albicans* disseminated infection model. Mice were infected with *C. albicans* isolate 0304103 and treated with vehicle, compounds **1**, **2** (**A**), **20a** (**B**), **20h** (**C**), **24** (**D**), FLC or the combination. *** $P < 0.001$, versus the FLC group by log-rank test for significance.

Preliminary PK Profiles. *In vitro* metabolic stability of compounds **20a**, **20h** and **24** was evaluated using the liver microsome assay. As shown in **Table 7**, compounds **20a**, **20h** and **24** exhibited similar metabolic properties with the half life of 19.4, 15.7 and 16.5 minutes, respectively. Furthermore, PK profiles of compound **20a** were evaluated in Sprague-Dawley (SD) rats. When it was administered *i.p* at 10 mg/kg, the half-life was approximately 5.14 h. The peak concentration C_{max} and plasma clearance (CL) was 1603.41 ng/mL and 2246.64 mL/h/mg, respectively (**Figure 10**).

Table 7. The mice microsomal stability of compounds **20a**, **20h** and **24**

	$T_{1/2}$[a](min)	CL[b] (mL/min/mg)
20a	19.4	0.0716
20h	15.7	0.0881
24	16.5	0.0838

[a] Half-life. [b] Clearance.

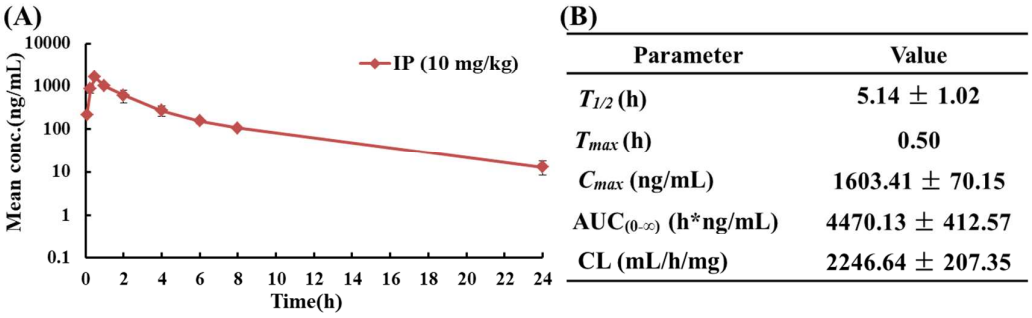

Figure 10. Pharmacokinetics of compound **20a** in rats. (**A**) Mean (± sd) plasma concentration-time profiles of compound **20a** in SD rats. (**B**) PK parameters of compound **20a**.

CONCLUSIONS

In summary, this study provided a novel strategy of for the combinational treatment of leukemia and IFIs by designing novel JAK2-HDAC dual inhibitors. In particular, compound **20a** was a highly active and selective JAK2/HDAC6 dual inhibitor that showed potent antiproliferative activity toward hematological cell lines and excellent synergistic effects with FLC to treat resistant *C. albicans*. Importantly, the therapeutic potential of compound **20a** was validated in several *in vivo* models. It showed good *in vivo* antitumor efficacy in the HEL xenograft model, significantly prolonged the survival of leukemic mice in the AML model, reduced leukemic infiltration to spleen,

and extended the survival of mice infected with resistant *C. albicans* in combination with FLC. To the best of our knowledge, this is the first example that a small molecule can simultaneously treat AML and synergize with FLC to treat resistant fungal infections. Further mechanism and lead optimization studies are in progress.

EXPERIMENTAL SECTION

Chemistry. *General methods.* ^{1}H NMR and ^{13}C NMR spectra were recorded on Bruker AVANCE300 or AVANCE600 spectrometers (Bruker Company, Germany), using TMS as an internal standard and $CDCl_3$ or DMSO-*d6* as solvents. Chemical shifts are given in ppm (δ). Elemental analyses were performed with a MOD-1106 instrument and were consistent with theoretical values within 0.4%. The mass spectra were recorded on an Esquire 3000 LC-MS mass spectrometer. Silica gel thin-layer chromatography was performed on precoated plates GF-254 (Qingdao Haiyang Chemical, China). All solvents and reagents were analytically pure, and no further purification was needed. All starting materials were commercially available. The purities of the compounds were determined by HPLC (Agilent 1260), and all final compounds exhibited purities greater than 95%.

1-(4-((4-(4-((cyanomethyl)carbamoyl)phenyl)pyrimidin-2-yl)amino)phenyl)-*N*-hydroxypiperidine-4-carboxamide (**8**). To a stirred solution of hydroxylamine hydrochloride (4.67 g, 67 mmol) in MeOH (24 mL) was added dropwise a solution of potassium hydroxide (5.61 g, 100 mmol) in MeOH (12 mL) at 0 °C. After addition, the mixture was stirred for 30 min at room temperature. The precipitate was filtered

and the filtrate formed a solution of free hydroxylamine in MeOH. Then, compound **7** (0.1 g, 0.20 mmol) was dissolved in above freshly prepared solution of hydroxylamine in MeOH (15 mL). The mixture was stirred at room temperature for 45 min, and then adjusted to pH 7 with acetic acid. The mixture was concentrated and the residue was washed with water to afford compound **8** (0.05 g, 53%) as a yellow solid. Mp: 213-215 ^{o}C. ^{1}H-NMR (DMSO-d_6, 600 MHz) δ: 10.43 (s, 1H), 9.42 (s, 1H), 9.04 (s, 1H), 8.81 (t, J = 5.67 Hz, 1H), 8.68 (s, 1H), 8.50 (d, J = 5.21 Hz, 1H), 8.22 (d, J = 8.51 Hz, 2H), 8.00 (d, J = 8.51 Hz, 2H), 7.62 (d, J = 9.16 Hz, 2H), 7.36-7.38 (m, 1H), 6.91 (d, J = 8.76 Hz, 2H), 5.37 (s, 1H), 3.88 (d, J = 6.07 Hz, 1H), 3.62 (d, J = 12.57 Hz, 2H), 2.56-2.61 (m, 2H), 2.09-2.13 (m, 1H), 1.67-1.72 (m, 4H). ^{13}C-NMR (150 MHz, DMSO-d_6, TMS) δ: 171.51, 166.27, 162.58, 160.34, 159.21, 150.47, 146.44, 139.36, 135.36, 132.35, 127.83, 127.77, 126.73, 126.68, 120.44, 116.45, 107.49, 49.16, 42.39, 28.03. MS (ESI negative): m/z $[M-H]^{+}$: 470.52.

***N*-(2-aminophenyl)-1-(4-((4-(4-((cyanomethyl)carbamoyl)phenyl)pyrimidin-2-yl) amino)phenyl)piperidine-4-carboxamide** (**10**). To a solution of compound **9** (0.11 g, 0.24 mmol), HATU (0.11 g, 0.29 mmol) and DIPEA (50 μL, 0.48 mmol) in DMF (5 mL) was added *o*-phenylenediamine (0.03 mg, 0.29 mmol), and the mixture was stirred at room temperature for 4 h. The reaction solution was diluted with water (40 mL) and filtered. The precipitate was dried and purified by column chromatography (CH_2Cl_2: MeOH = 100: 3) to give target compound **10** (0.07 g, 51%) as a yellow solid. Mp: 154-156 ^{o}C.^{1}H-NMR (DMSO-d_6, 600 MHz) δ: 10.00 (s, 4H), 9.47 (s, 1H), 9.41 (t, J = 5.41 Hz, 1H), 9.19 (s, 1H), 8.54 (d, J = 5.41 Hz, 1H), 8.27 (d, J = 8.50 Hz, 2H),

8.04 (d, *J* = 8.50 Hz, 2H), 7.66 (d, *J* = 8.50 Hz, 2H), 7.40 (d, *J* = 5.41 Hz, 1H), 7.19 (d, *J* = 6.96 Hz, 1H), 6.97 (s, 2H), 6.89 (t, *J* = 6.96 Hz, 1H), 6.72 (d, *J* = 6.96 Hz, 1H), 6.54 (t, *J* = 6.96 Hz, 1H), 4.88 (s, 1H), 4.35 (d, *J* = 5.22 Hz, 2H), 3.68 (d, *J* = 11.48 Hz, 2H), 2.69 (s, 2H), 2.56 (s, 1H), 1.92 (d, *J* = 12.01, 2H), 1.80 (d, *J* = 12.01 Hz, 2H). ^{13}C-NMR (DMSO-d_6, 150 MHz) δ: 166.17, 162.42, 160.30, 159.28, 139.92, 134.50, 127.90, 126.94, 125.75, 125.35, 123.03, 120.34, 117.54, 116.83, 116.40, 116.03, 111.10, 107.67, 62.72, 49.45, 28.20, 27.73. MS (ESI positive): m/z $[M+H]^+$: 547.55.

(*E*)-1-(4-((4-(4-((cyanomethyl)carbamoyl)phenyl)pyrimidin-2-yl)amino)phenyl)-*N*-(4-(3-(hydroxyamino)-3-oxoprop-1-en-1-yl)phenyl)piperidine-4-carboxamide (**12a**). To a stirred solution of compound **9** (0.12 g, 0.26 mmol), HATU (0.12 g, 0.32 mmol) and DIPEA (84 μL, 0.52 mmol) in DMF (5 mL) was added *(E)*-methyl 3-(4-aminophenyl)acrylate (0.04 mg, 0.32 mmol), and the mixture was stirred at room temperature for 4 h. The reaction solution was diluted with water (40 mL) and filtered. The precipitate was dried and purified by column chromatography (CH_2Cl_2: MeOH = 100: 4) to give intermediate **11a** (0.097 g, 61%) as a yellow solid. ^{1}H-NMR (DMSO-d_6, 600 MHz) δ: 10.16 (s, 1H), 9.49 (s, 1H), 9.35 (t, *J* = 5.22 Hz, 1H), 8.56 (d, *J* = 5.32 Hz, 1H), 8.29 (d, *J* = 8.40 Hz, 2H), 8.05 (d, *J* = 8.40 Hz, 2H), 7.70 (d, *J* = 6.67 Hz, 3H), 7.67 (d, *J* = 5.32 Hz, 1H), 7.62 (d, *J* = 16.08 Hz, 1H), 7.42 (d, *J* = 5.14 Hz, 1H), 6.98 (d, *J* = 8.46 Hz, 2H), 6.54 (d, *J* = 16.08 Hz, 1H), 4.38 (d, *J* = 5.32 Hz, 2H), 3.73 (s, 3H), 3.71 (d, *J* = 13.18 Hz, 2H), 2.69 (t, *J* = 10.01 Hz, 2H), 1.92 (d, *J* = 11.26 Hz, 2H), 1.79-1.83 (m, 2H). MS (ESI positive): m/z $[M+H]^+$: 616.23.

Compound **11a** (0.08 g, 0.13 mmol) was dissolved in above freshly prepared solution

of hydroxylamine in MeOH (15 mL). The mixture was stirred at room temperature for 45 min, and then adjusted to pH 7 with acetic acid. The mixture was concentrated and the residue was washed with water to afford target compound **12a** (0.05 g, 62%) as a yellow solid. Mp: 244-246 °C. ^{1}H-NMR (DMSO-d_6, 600 MHz) δ: 10.10 (s, 1H), 9.45 (s, 1H), 8.52 (d, J = 4.84 Hz, 1H), 8.24 (d, J = 7.87 Hz, 2H), 8.03 (t, J = 7.87 Hz, 2H), 7.68 (t, J = 8.48 Hz, 4H), 7.50 (d, J = 8.48 Hz, 1H), 7.39 (d, J = 5.45 Hz, 2H), 6.96 (d, J = 8.48 Hz, 2H), 6.38 (t, J = 15.74 Hz, 1H), 5.39 (s, 1H), 3.90 (d, J = 6.01 Hz, 1H), 3.68-3.71 (m, 2H), 2.67 (t, J = 10.58 Hz, 2H), 1.90 (d, J = 11.90 Hz, 2H), 1.78-1.82 (m, 2H). ^{13}C-NMR (DMSO-d_6, 150 MHz) δ: 173.69, 166.20, 166.01, 162.54, 160.33, 159.19, 150.44, 146.45, 139.35, 135.77, 132.45, 129.06, 128.13, 127.85, 127.77, 126.73, 126.67, 120.40, 119.16, 119.05, 117.19, 116.51, 107.50, 49.18, 42.74, 28.91, 28.14. MS (ESI positive): m/z $[M+MeOH]^+$: 650.61.

Compound **12b** was synthesized according to a similar protocol described for **12a**.

***N*-(4-(hydroxycarbamoyl)phenyl)-1-(4-((4-(4-(methylsulfonamido)phenyl)pyrimidin-2-yl)amino)phenyl)piperidine-4-carboxamide** (**12b**). Yield 58%, yellow solid. Mp: 276-278 °C. ^{1}H-NMR (DMSO-d_6, 600 MHz) δ: 11.11 (s, 1H), 10.30 (s, 1H), 9.43 (d, J = 8.61 Hz, 1H), 8.52 (t, J = 6.40 Hz, 1H), 8.26 (d, J = 8.54 Hz, 1H), 8.23 (d, J = 8.54 Hz, 1H), 8.01-8.03 (m, 2H), 7.91 (d, J = 8.54 Hz, 1H), 7.76 (d, J = 8.54 Hz, 1H), 7.69 (d, J = 8.54 Hz, 1H), 7.64 (d, J = 8.54 Hz, 2H), 7.37-7.42 (m, 1H), 6.96 (d, J = 8.54 Hz, 2H), 5.39 (s, 1H), 4.34 (d, J = 4.00 Hz, 1H), 3.82 (s, 3H), 3.69 (d, J = 12.00 Hz, 2H), 2.67 (t, J = 12.00 Hz, 2H), 1.91 (d, J = 12.00 Hz, 2H), 1.75-1.81 (m, 2H). ^{13}C-NMR (DMSO-d_6, 150 MHz) δ: 174.02, 170.87, 166.12, 165.80, 162.59, 162.40,

160.35, 159.25, 159.17, 150.40, 146.44, 143.75, 139.96, 139.35, 135.81, 134.51, 132.53, 130.30, 130.20, 127.88, 127.78, 127.61, 126.93, 126.71, 126.66, 123.70, 120.37, 118.45, 118.34, 117.56, 116.52, 107.55, 107.49, 51.81, 49.17, 42.79, 28.93, 28.12, 27.75. MS (ESI positive): m/z $[M+H]^+$: 590.52.

Compounds **16**, **18**, **20a-h** were synthesized according to a similar protocol described for compounds **8**, **10** and **12a**, respectively.

***N*-hydroxy-1-(4-((4-(4-(methylsulfonamido)phenyl)pyrimidin-2-yl)amino)phenyl) piperidine-4-carboxamide** (**16**). Yield 72%, light yellow solid. Mp: 213-215 ^oC. ^1H-NMR (DMSO-d_6, 600 MHz) δ: 11.35 (s, 1H), 10.28 (s, 1H), 8.62 (s, 1H), 7.98 (t, J = 5.47 Hz, 1H), 7.92 (d, J = 7.75 Hz, 1H), 7.56 (t, J = 7.75 Hz, 1H), 7.49 (d, J = 7.75 Hz, 1H), 7.37 (d, J = 7.75 Hz, 1H), 7.24 (d, J = 7.75 Hz, 1H), 7.17 (t, J = 7.29 Hz, 1H), 7.13 (t, J = 7.29 Hz, 1H), 7.03 (t, J = 7.29 Hz, 1H), 6.18 (s, 1H), 5.34 (d, J = 5.93 Hz, 1H), 3.37 (d, J = 15.50 Hz, 1H), 3.17 (s, 1H), 3.09-3.12 (m, 1H), 2.87-2.91 (m, 2H), 2.51 (s, 3H), 1.84 (t, J = 7.33 Hz, 2H), 1.28-1.34 (m, 2H), 1.18-1.24 (m, 2H), 1.00-1.04 (m, 4H). ^{13}C-NMR (DMSO-d_6, 150 MHz) δ: 171.50, 162.78, 160.24, 128.77, 146.28, 140.79, 132.59, 131.68, 128.02, 120.26, 118.75, 116.51, 106.59, 49.23, 45.72, 28.05, 8.53. MS (ESI positive): m/z $[M+H]^+$: 483.51.

***N*-(2-aminophenyl)-1-(4-((4-(4-(methylsulfonamido)phenyl)pyrimidin-2-yl)amino)phenyl)piperidine-4-carboxamide** (**18**). Yield 63%, yellow solid. Mp: 220-222 ^oC. ^1H-NMR (DMSO-d_6, 600 MHz) δ: 10.12 (s, 1H), 9.34 (s, 1H), 9.11 (s, 1H), 8.42 (d, J = 5.24 Hz, 1H), 8.11 (d, J = 8.64 Hz, 2H), 7.64 (d, J = 8.64 Hz, 2H), 7.31 (d, J = 8.64 Hz, 2H), 7.24 (d, J = 5.55 Hz, 1H), 7.16 (d, J = 8.02 Hz, 1H), 6.94 (d, J = 9.26 Hz,

2H), 6.88 (t, *J* = 7.40 Hz, 1H), 6.70 (d, *J* = 8.02 Hz, 1H), 4.80 (s, 2H), 3.67 (d, *J* = 12.34 Hz, 2H), 3.05 (s, 3H), 2.64 (t, *J* = 13.57 Hz, 2H), 1.89 (d, *J* = 12.34 Hz, 2H), 1.73-1.80 (m, 2H). ^{13}C-NMR (DMSO-d_6, 150 MHz) δ: 173.38, 162.82, 160.26, 158.74, 146.37, 141.88, 141.15, 132.64, 131.48, 128.01, 125.71, 125.32, 123.44, 120.20, 118.68, 116.51, 116.17, 115.88, 106.53, 49.29, 42.11, 28.43. MS (ESI positive): m/z $[M+H]^+$: 558.48.

(*E*)-*N*-(4-(3-(hydroxyamino)-3-oxoprop-1-en-1-yl)phenyl)-1-(4-((4-(4-(methylsulfonamido)phenyl)pyrimidin-2-yl)amino)phenyl)piperidine-4-carboxamide (**20a**). Yield 58%, yellow solid. Mp: 239-241 ^{o}C. ^{1}H-NMR (DMSO-d_6, 600 MHz) δ: 10.70 (s, 1H), 10.13 (s, 1H), 9.33 (s, 1H), 8.43 (d, *J* = 5.29 Hz, 1H), 8.11 (d, *J* = 9.07 Hz, 3H), 7.63-7.39 (m, 5H), 7.48 (d, *J* = 8.66 Hz, 2H), 7.37 (d, *J* = 15.24 Hz, 1H), 7.33 (d, *J* = 9.70 Hz, 2H), 7.25 (d, *J* = 4.94 Hz, 1H), 6.94 (d, *J* = 8.95 Hz, 2H), 6.35 (d, *J* = 15.68 Hz, 1H), 3.67 (d, *J* = 13.10 Hz, 3H), 3.07 (s, 3H), 2.64 (t, *J* = 12.08 Hz, 2H), 1.88 (d, *J* = 11.72 Hz, 2H), 1.73-1.79 (m, 2H). ^{13}C-NMR (DMSO-d_6, 150 MHz) δ: 173.71, 163.15, 162.81, 160.28, 158.76, 146.25, 140.79, 140.52, 132.69, 131.75, 128.13, 128.01, 120.25, 119.17, 118.75, 117.16, 116.54, 106.59, 49.20, 42.71, 28.91, 28.15. HRMS (ESI, negative) m/z calcd for $C_{32}H_{32}N_7O_5S$ (M - H): 626.2191; found 626.2202. HPLC purity: 97.0%.

***N*-(4-(hydroxycarbamoyl)phenyl)-1-(4-((4-(4-(methylsulfonamido)phenyl)pyrimidin-2-yl)amino)phenyl)piperidine-4-carboxamide** (**20b**). Yield 62%, yellow solid. Mp: 229-231 ^{o}C. ^{1}H-NMR (DMSO-d_6, 600 MHz) δ: 10.17 (s, 1H), 9.37 (s, 1H), 8.46 (d, *J* = 4.92 Hz, 1H), 8.14 (d, *J* = 8.85 Hz, 2H), 7.67-7.74 (m, 5H), 7.33 (d, *J* = 8.36

Hz, 2H), 7.28 (d, *J* = 5.01 Hz, 1H), 6.98 (d, *J* = 8.36 Hz, 2H), 3.71 (d, *J* = 11.70 Hz, 2H), 3.08 (s, 3H), 2.68 (t, *J* = 11.87 Hz, 2H), 1.92 (d, *J* = 11.82 Hz, 2H), 1.78-1.84 (m, 2H). ^{13}C-NMR (DMSO-d_6, 150 MHz) δ: 173.79, 163.83, 162.85, 160.25, 158.69, 146.30, 141.86, 141.55, 132.72, 131.21, 127.99, 127.59, 126.99, 120.18, 118.69, 118.36, 116.55, 106.50, 49.23, 42.76, 28.19. MS (ESI positive): m/z $[M+H]^+$: 602.46.

***N*-(4-(hydroxycarbamoyl)benzyl)-1-(4-((4-(4-(methylsulfonamido)phenyl)pyrimidin-2-yl)amino)phenyl)piperidine-4-carboxamide** (**20c**). Yield 57%, light yellow solid. Mp: 207-209 °C. ^{1}H-NMR (DMSO-d_6, 600 MHz) δ: 11.17 (s, 1H), 9.35 (s, 1H), 9.03 (s, 1H), 8.46 (d, *J* = 5.72 Hz, 1H), 8.42 (t, *J* = 5.72 Hz, 1H), 8.14 (d, *J* = 8.57 Hz, 2H), 7.72 (d, *J* =8.57 Hz, 2H), 7.67 (d, *J* = 8.57 Hz, 2H), 7.32-7.40 (m, 4H), 7.28 (d, *J* = 5.72 Hz, 1H), 6.96 (d, *J* = 8.57 Hz, 2H), 4.39 (d, *J* = 5.72 Hz, 2H), 3.67 (d, *J* = 11.68 Hz, 2H), 3.10 (s, 3H), 2.65 (t, *J* = 10.99 Hz, 2H), 2.34-2.36H (m, 1H), 1.85 (d, *J* = 13.19 Hz, 2H), 1.73-1.80 (m, 2H). ^{13}C-NMR (DMSO-d_6, 150 MHz) δ: 174.13, 169.12, 162.78, 160.25, 158.75, 146.39, 140.87, 132.56, 131.63, 128.01, 126.83, 120.19, 118.68, 116.46, 106.54, 49.29, 41.82, 38.28, 32.20, 29.03, 28.48, 28.37, 26.20, 25.01. MS (ESI positive): m/z $[M+H]^+$: 616.52.

***N*-(4-(hydroxyamino)-4-oxobutyl)-1-(4-((4-(4-(methylsulfonamido)phenyl)pyrimidin-2-yl)amino)phenyl)piperidine-4-carboxamide** (**20d**). Yield 68%, yellow solid. Mp: 221-223 °C. ^{1}H-NMR (DMSO-d_6, 600 MHz) δ: 10.33 (s, 1H), 10.11 (s, 1H), 9.31 (s, 1H), 8.65 (s, 1H), 8.43 (d, *J* = 4.41 Hz, 1H), 8.11 (d, *J* = 8.81 Hz, 2H), 7.79 (t, *J* = 5.32 Hz, 1H), 7.63 (d, *J* = 8.65 Hz, 2H), 7.32 (d, *J* = 8.65 Hz, 2H), 7.24 (d, *J* = 4.66 Hz, 1H), 6.91 (d, *J* = 8.65 Hz, 2H), 3.61 (d, *J* = 12.64 Hz, 2H), 3.07 (s, 3H), 3.00-3.03

(m, 2H), 2.58 (t, J = 10.64 Hz, 2H), 2.17-2.21 (m, 1H), 1.93 (t, J = 7.98 Hz, 2H), 1.74 (d, J = 10.64 Hz, 2H), 1.68 (t, J = 9.31 Hz, 2H), 1.58-1.64 (m, 2H). ^{13}C-NMR (DMSO-d_6, 150 MHz) δ: 174.27, 168.85, 162.78, 160.25, 158.76, 146.38, 140.83, 132.58, 131.66, 128.02, 120.19, 118.67, 116.48, 106.55, 49.29, 41.82, 38.03, 29.84, 28.32, 25.32. MS (ESI positive): m/z $[M+H]^+$: 568.50.

***N*-(5-(hydroxyamino)-5-oxopentyl)-1-(4-((4-(4-(methylsulfonamido)phenyl)pyrimidin-2-yl)amino)phenyl)piperidine-4-carboxamide** (**20e**). Yield 56%, light yellow solid. Mp: 204-206 ^{o}C. ^{1}H-NMR (DMSO-d_6, 600 MHz) δ: 10.32 (s, 1H), 10.16 (s, 1H), 9.32 (s, 1H), 8.65 (s, 1H), 8.43 (d, J = 4.55 Hz, 1H), 8.11 (d, J = 7.96 Hz, 2H), 7.78 (s, 1H), 7.64 (d, J = 8.53 Hz, 2H), 7.31 (d, J = 7.96 Hz, 2H), 7.25 (d, J = 4.55 Hz, 1H), 6.92 (d, J = 8.53 Hz, 2H), 3.62 (d, J = 10.23 Hz, 2H), 3.06 (s, 3H), 3.02-3.04 (m, 2H), 2.59 (t, J = 10.23 Hz, 2H), 2.21 (t, J = 11.37 Hz, 2H), 1.94 (t, J = 6.82 Hz, 2H), 1.67-1.73 (m, 4H), 1.47 (t, J = 6.82 Hz, 2H), 1.36 (t, J = 6.82 Hz, 2H). ^{13}C-NMR (DMSO-d_6, 150 MHz) δ: 174.12, 169.12, 162.78, 160.25, 158.75, 146.35, 140.84, 132.61, 131.66, 128.01, 120.19, 118.68, 116.49, 106.55, 49.32, 41.79, 38.28, 32.20, 29.03, 28.48, 28.35, 26.20, 25.01.MS (ESI positive): m/z $[M+H]^+$: 582.51.

***N*-(6-(hydroxyamino)-6-oxohexyl)-1-(4-((4-(4-(methylsulfonamido)phenyl)pyrimidin-2-yl)amino)phenyl)piperidine-4-carboxamide** (**20f**). Yield 65%, yellow solid. Mp: 170-172 ^{o}C. ^{1}H-NMR (DMSO-d_6, 600 MHz) δ: 10.32 (s, 1H), 9.27 (s, 1H), 8.39 (d, J = 4.75 Hz, 1H), 8.05 (d, J = 7.92 Hz, 2H), 7.65 (s, 1H), 7.45 (d, J = 7.92 Hz, 2H), 7.33 (d, J = 7.92 Hz, 2H), 7.20 (d, J = 4.75 Hz, 1H), 6.92 (d, J = 7.92 Hz, 2H), 3.62 (d, J = 10.57 Hz, 2H), 3.00-3.03 (m, 4H), 2.96 (t, J = 10.23 Hz, 2H), 2.69 (s, 1H), 2.59 (t,

J = 10.57 Hz, 2H), 2.21 (s, 1H), 1.93 (t, *J* = 5.28 Hz, 2H), 1.68-1.73 (m, 4H), 1.49 (t, *J* = 7.92 2H), 1.35-1.39 (m, 2H). ^{13}C-NMR (DMSO-d_6, 150 MHz) δ: 174.07, 168.97, 163.09, 160.22, 158.42, 146.31, 133.05, 132.74, 132.37, 131.47, 131.41, 128.75, 128.67, 127.85, 127.08, 120.09, 118.81, 116.48, 106.22, 49.35, 41.82, 38.22, 32.18, 28.85, 28.28, 25.96, 24.83. MS (ESI positive): m/z $[M+H]^+$: 596.94.

***N*-(7-(hydroxyamino)-7-oxoheptyl)-1-(4-((4-(4-(methylsulfonamido)phenyl)pyrimidin-2-yl)amino)phenyl)piperidine-4-carboxamide** (**20g**). Yield 63%, yellow solid. Mp: 183-185 °C. ^{1}H-NMR (DMSO-d_6, 600 MHz) δ: 10.33 (s, 1H), 10.14 (s, 1H), 9.35 (s, 1H), 8.65 (s, 1H), 8.47 (d, *J* = 5.19 Hz, 1H), 8.15 (d, *J* = 8.30 Hz, 2H), 7.73 (t, *J* = 5.19 Hz, 1H), 7.66 (d, *J* = 8.30 Hz, 2H), 7.36 (d, *J* = 8.30 Hz, 2H), 7.28 (d, *J* = 5.19 Hz, 1H), 6.95 (d, *J* = 8.30 Hz, 2H), 3.64 (d, *J* = 11.41 Hz, 2H), 3.11 (s, 3H), 3.03-3.07 (m, 2H), 2.62 (t, *J* = 9.34 Hz, 2H), 2.23 (s, 1H), 1.95 (t, *J* = 8.35 Hz, 2H), 1.76 (t, *J* = 10.31 Hz, 2H), 1.71 (d, *J* = 10.31 Hz, 2H), 1.50 (t, *J* = 8.25 Hz, 2H), 1.39-1.51 (m, 2H). ^{13}C-NMR (DMSO-d_6, 150 MHz) δ: 174.11, 169.10, 160.26, 146.39, 140.84, 132.57, 131.66, 128.02, 120.19, 118.67, 116.47, 106.55, 49.31, 41.82, 38.27, 32.19, 28.97, 28.36, 28.26, 26.04, 25.04. MS (ESI positive): m/z $[M+H]^+$: 610.83.

***N*-(8-(hydroxyamino)-8-oxooctyl)-1-(4-((4-(4-(methylsulfonamido)phenyl)pyrimidin-2-yl)amino)phenyl)piperidine-4-carboxamide** (**20h**). Yield 65%, yellow solid. Mp: 199-201 °C. ^{1}H-NMR (DMSO-d_6, 600 MHz) δ: 10.33 (s, 1H), 9.35 (s, 1H), 8.65 (s, 1H), 8.46 (d, *J* = 5.48 Hz, 1H), 8.14 (d, *J* = 8.22 Hz, 2H), 7.77 (t, *J* = 5.48 Hz, 1H), 7.66 (d, J = 8.22 Hz, 2H), 7.35 (d, *J* = 8.22 Hz, 2H), 7.27 (d, *J* = 5.48 Hz, 1H), 6.95 (d, *J* = 8.22 Hz, 2H), 3.64 (d, *J* = 12.33 Hz, 2H), 3.09 (s, 3H), 3.03-3.07 (m, 3H), 2.61 (t,

J = 9.59 Hz, 2H), 2.21 (s, 1H), 1.95 (t, *J* = 7.85 Hz, 2H), 1.69-1.77 (m, 4H), 1.50 (t, *J* = 7.85 Hz, 2H), 1.36-1.40 (m, 2H). ^{13}C-NMR (DMSO-d_6, 150 MHz) δ: 174.08, 169.09, 162.77, 160.25, 158.74, 146.37, 140.84, 132.58, 131.65, 128.01, 120.17, 118.66, 116.46, 106.54, 49.30, 41.81, 38.28, 32.21, 29.05, 28.49, 28.37, 26.21, 25.02. HRMS (ESI, negative) m/z calcd for $C_{31}H_{40}N_7O_5S$ (M - H): 622.2817; found 622.2821. HPLC purity: 99.4%.

Compounds **24** and **26** were synthesized according to a similar protocol described for compounds **8** and **10**, respectively.

***N*-hydroxy-4-(2-((4-morpholinophenyl)amino)pyrimidin-4-yl)benzamide** (**24**). Yield 72%, light yellow solid. Mp: 176-178 °C. ^{1}H-NMR (DMSO-d_6, 600 MHz) δ: 11.32 (s, 1H), 8.50 (d, *J* = 5.17 Hz, 1H), 8.19 (d, *J* = 8.05 Hz, 2H), 7.88 (d, *J* = 8.05 Hz, 2H), 7.64 (d, *J* = 8.62 Hz, 2H), 7.35 (d, *J* = 5.17 Hz, 1H), 6.91 (d, *J* = 9.05 Hz, 2H), 3.72 (t, *J* = 4.67 Hz, 4H), 3.03 (t, *J* = 4.67 Hz, 4H). ^{13}C-NMR (DMSO-d_6, 150 MHz) δ: 162.59, 160.33, 159.17, 146.20, 139.19, 134.59, 132.83, 132.00, 131.47, 131.41, 129.61, 128.75, 128.68, 127.34, 126.79, 120.32, 115.60, 107.49, 66.15, 49.25. HRMS (ESI, negative) m/z calcd for $C_{21}H_{20}N_5O_3$ (M - H): 390.1572; found 390.1567. HPLC purity: 99.5%.

***N*-(2-aminophenyl)-4-(2-((4-morpholinophenyl)amino)pyrimidin-4-yl)benzamide** (**26**). Yield 60%, yellow solid. Mp: 206-208 °C. ^{1}H-NMR (DMSO-d_6, 600 MHz) δ: 9.76 (s, 1H), 9.49 (s, 1H), 8.52 (d, *J* = 4.81 Hz, 1H), 8.26 (d, *J* = 8.17 Hz, 2H), 8.12 (d, *J* = 8.17 Hz, 2H), 7.66 (d, *J* = 9.13 Hz, 2H), 7.41 (d, *J* = 4.81 Hz, 1H), 7.18 (d, *J* = 7.21 Hz, 1H), 6.97 (t, *J* = 7.21 Hz, 1H), 6.92 (d, *J* = 9.13 Hz, 2H), 6.78 (d, *J* = 8.17

Hz, 1H), 6.59 (t, J = 7.21 Hz, 1H), 4.93 (s, 2H), 3.73 (t, J = 4.74 Hz, 4H), 3.04 (t, J = 4.74 Hz, 4H). ^{13}C-NMR (DMSO-d_6, 150 MHz) δ: 164.77, 162.59, 160.35, 159.21, 146.21, 143.18, 139.38, 136.44, 132.85, 128.27, 126.67, 123.10, 120.33, 116.20, 116.07, 115.60, 107.56, 66.15, 49.25. MS (ESI positive): m/z $[M+H]^+$: 483.33.

***In vitro* JAK Inhibition Assay.** The kinase assay was performed in the buffer (50 mM HEPES, pH 7.5, 0.015% Brij-35, 10 mM $MgCl_2$, 10 mM $MnCl_2$, 2 mM DTT). A 5 mL volume of tested compounds (3-fold dilution, 10 concentrations) were prediluted for dose response in 384-well plates in duplicates. A 10 mL volume of diluted enzyme solution was sequentially added and the assay plates were incubated at room temperature for 10 min. Then, a 10 mL volume of a mixture of peptide solution containing FAM-labeled peptide (GL Biochem, Cat. No. 112393, Lot. No. P130408-ZB112393, China) and ATP (Sigma, Cat. No. A7699-1G, CAS No. 987-65-5, America) was incubated at 28 °C for 25 min. Reaction was stopped with the addition of 50 mM EDTA containing 25 mL of 100 mM HEPES, pH 7.5, 0.015% Brij-35, and 0.2% Coating Reagent #3, and the data were collected on Caliper. Half maximal inhibition (IC_{50}) values were calculated using a nonlinear curve fit with XLfit software.

***In vitro* HDAC Inhibition Assay.** The HDAC1 (#AB101661) and HDAC6 (#AB42632) enzymes were purchased from Abcam. HDAC3 (#BML-SE515-0050) was purchased from ENZO Inc. HDAC4 (#H86-31G) and HDAC8 (#H90-30H) was purchased from SignalChem. The reaction mixture contained 25 mM Tris (pH 8.0), 1 mM $MgCl_2$, 0.1 mg/mL BSA, 137mM NaCl, 2.7 mM KCl, HDAC (HDAC1, 7.2

ng/well; HDAC2, 7.5 ng/well; HDAC3, 3.4 ng/well; HDAC4, 0.3 ng/well; HDAC6, 15 ng/well; HDAC8, 22 ng/well) in a total volume of 40 μL. The test compounds (3-fold dilution, 10 concentrations) were diluted in 10% DMSO and 5 μL of the dilution was added and preincubated with purified recombinant HDAC at room temperature for 5 min before substrate addition. Finally, the enzyme substrate (Ac-Leu-Gly-Lys(Ac)-AMC, 10 μM for HDAC1, 2, 3, 6; Ac-Leu-Gly-Lys(Tfa)-AMC, 2 μM for HDAC4 and HDAC8) was added and the plate was incubated at 37 ℃ for 30 min in a final volume of 50 μL. The reaction was quenched with 50 μL HDAC assay developer (1 mg/mL trypsin and 2 μM TSA in assay buffer) for 30 min at room temperature. The assay was performed by quantitating the fluorescent product amount of in solution following an enzyme reaction. Fluorescence was then analyzed with an excitation of 350-360 nm and an emission wavelength of 450-460 nm at Spectra Max M5 microtiter plate reader. The IC_{50} values were calculated using nonlinear regression with normalized dose-response fit using Prism GraphPad software. All experiments were independently performed at least three times.

***In vitro* Antiproliferative Assay.** Three human leukemic cell lines, HL60, K562 and HEL, which were in the logarithmic phase, were harvested and plated in cells were plated in 96-well transparent plates at a density of 7×10^3/well and incubated in a humidified atmosphere with 5% CO_2 at 37 ℃ for 24 h. Test compounds were added onto triplicate wells with different concentrations and 0.1% DMSO for control. After they had been incubated for 48 h, 10 μL of cell counting kit-8 (CCK8) solution was added to each well and the plate was incubated for additional 1-4 h. The absorbance

(OD) was read on a Biotek Synergy H2 (Lab systems) at 450 nm. The concentration causing 50% inhibition of cell growth (IC_{50}) was determined by the Logit method. All experiments were performed three times.

Checkerboard Microdilution Assay. Assays were performed according to the methods of the CLSI (formerly NCCLS) (M27-A). Briefly, RPMI 1640 medium was adjusted to pH 7 at 25 °C using 3-[*N*-morpholino]-propanesulphonic acid (MOPS). The initial concentration of the fungal suspension in RPMI 1640 medium was 10^3 CFU/mL, and the final concentrations ranged from 0.125 μg/mL to 64 μg/mL for FLC and 1 μg/mL to 32 μg/mL for target compounds in the 96-well microtiter plates. A drug-free medium with fungi and a fungus-free medium were used as the positive and negative controls, respectively. Plates were incubated at 35 °C for 48 h. OD was measured at 630 nm, and background OD was subtracted from that of each well. MIC_{50} was determined as the lowest concentration of the drugs (alone or in combination) that inhibited cell growth by 50%, compared with the cell growth of the drug-free wells. The fractional inhibitory concentration (FIC) index is defined as the sum of the MIC of each drug used in combination divided by the MIC of the drug used alone. Synergy and antagonism were defined by FIC index of ≤ 0.5 and >4, respectively. An FIC index >0.5 but ≤ 4 was considered indifferent.

Apoptosis Detection Assay. HEL cells (3×10^5 cells/mL) were seeded in six-well plates and treated with compounds **20a**, **20h** and **24** at concentration of 5 μM and 10 μM for 48 h. The cells were then harvested by trypsinization and washed twice with cold PBS. After centrifugation and removal of the supernatants, cells were

resuspended in 400 μL of 1 x binding buffer which was then added to 5 μL of annexin V-FITC and incubated at room temperature for 15 min. After adding 10 μL of PI the cells were incubated at room temperature for another 15 min in dark. The stained cells were analyzed by a Flow Cytometer (BD Accuri C6).

Cell Cycle Analysis by Flow Cytometry. HEL cells (3×10^5 cells/well) were treated with compounds **20a**, **20h** and **24** at different concentration for 48 h. The treated cells were collected, resuspended, and then, incubated for 30 min at 37 °C with 25 μg/mL PI and 10 μg/mL RNase buffer. For each sample, at least 1 x 10^4 cells were analyzed using flow cytometry (BD Accuri C6).

Western Blotting. HEL cells were seeded (5×10^5 cells/well) on 6-well transparent plates (Corning). HEL cells were exposed to compounds **20a**, **20h** and **24** at 0.2, 1 and 5 μM for 24 h and then harvested and washed with PBS three times. Then the cells were lysed with RIPA Cell Lysis Buffer on ice for 30 min. The cell lysates were centrifuged at 12000 x g for 15 min at 4 ^{o}C. Supernatant was collected and BCA Protein Assay was used for determined protein concentration. Equal amounts of protein (30 μg) were separated by SDS-PAGE. Then the proteins were transferred to polyvinylidene fluoride membranes and were blocked with 5% BSA for 2 h. The membranes were incubated with the primary antibody overnight at 4 °C and were washed with TBST for three times. Then the mixture was incubated with the secondary antibody for 1.5 h. The membranes were washed with TBST for three times. The immunoblots were visualized by Odyssey Infrared Imaging. The antibodies including anti-Histone H3 (#ab1791, Abcam), anti-Histone H4 (#ab9051, Abcam),

anti- STAT5 (phosphor Y694, #ab32364, Abcam) were purchased from Abcam.

Growth Curve Assay. Growth curve assay was performed according to the reported protocol,[55] with a few modifications. Briefly, exponentially growing *C. albicans* cells were harvested and resuspended in fresh YPD medium to a concentration of 5 x 10^4 cells/mL. Various concentrations of FLC and compounds **20a**, **20h** and **24** were added. The cells were cultured at 30 °C with constant shaking (20 r.p.m.) and counted at designated time points after culture (0, 4, 8, 12 and 24 h). No FLC or selected compounds were added in the control group. Three independent experiments were performed.

***In vitro* Biofilm Formation Assay**. Biofilm formation assay was performed in a 96-well tissue culture plate (Corning, cat. no. 3599) by seeding with 100 μL cell suspensions (1×10^6 cells/mL) in RPMI 1640 medium, and incubating them with 64 μg/mL of FLC statically at 37 °C. After 90 min adhesion, the medium was aspirated, non-adherent cells were removed, and different concentration of compounds **20a**, **20h** and **24** was added. The plate was further incubated at 37 °C for 24 h. A semiquantitative measure of the formed biofilms was calculated using an XTT reduction assay.

HEL Xenograft Tumor Mouse Model. The experimental procedures and the animal use and care protocols were approved by the Committee on Ethical Use of Animals of Second military medical university. BALB/C nude female mice (Certificate SCXK-2007-0005, weighing 18 g to 20 g) were obtained from Shanghai Experimental Animal Center, Chinese Academy of Sciences. HEL cell suspensions were implanted

subcutaneously into the right axilla region of mice. Treatment was begun when implanted tumors had reached a volume of about 100-300 mm^3. The animals were randomized into appropriate groups (five animals) for the test of compounds **20a**, **20h** and **24**, and control mice received vehicle (0.5% carboxymethyl cellulose). Compounds were suspended in the 0.5% carboxymethyl cellulose and administered ip at the dose of 10 mg/kg/day for 21 consecutive days. Tumor volumes were monitored by caliper measurement of the length and width and calculated using the formula of $TV = 1/2 \times a \times b^2$, where a is the tumor length and b is the width. Tumor volumes and body weights were monitored every 2 days over the course of treatment. Mice were sacrificed on day 30 to 33 after implantation of cells and tumors were removed and recorded for analysis.

AML Mouse Model. 5×10^6 HEL cells were injected *via* tail vein to sublethally irradiated female 5-week SCID mice. The leukemic mice were randomized into appropriate groups (ten animals). Compounds were injected intraperitoneally at dose of 10 mg/kg every day. The leukemic mice become moribund and then were killed and the enlarged spleens were picked for histological assessments.

***In vivo* Antifungal Potency.** Female ICR mice 4 to 6 weeks old and weighing 20 to 25 g were housed and fed. After acclimatization for 1 week, mice were infected through the tail vein with 0.2 mL of yeast suspension, which corresponded to 15×10^4 CFU per mouse. FLC (at dose of 1 mg/kg) and compounds **20a**, **20h** and **24** (at dose of 5 mg/kg) were injected intraperitoneally alone or combination every day after the infection. The control group consisted of mice treated with placebo consisting of 0.5%

carboxymethyl cellulose. Survival was monitored daily and moribund mice were sacrificed and considered deceased at the time of sacrifice.

Supporting Information

Additional synthesis of intermediates, HPLC spectra for representative compounds, figures of proposed binding mode of compound **26**, the change of body weight of the nude mice in HEL xenograft model, the dissected spleen of leukemic mice, biological evaluations for selective HDAC3 and HDAC6 inhibitors, methods for pharmacokinetic studies and molecular docking and Molecular Formula Strings of the target compounds.

The Supporting Information is available free of charge on the ACS Publications website at DOI: XXXXXX/acs.jmedchem.XXXXXXX.

■ AUTHOR INFORMATION

Corresponding Author

* (C. S.) Phone / Fax: +86 21 81871239. E-mail: shengcq@smmu.edu.cn

Author Contributions

† S. H., G. D. and H. L. contributed equally to this work.

The manuscript was written through contributions of all authors. All authors have given approval to the final version of the manuscript.

Notes

The authors declare no competing financial interest.

■ ACKNOWLEDGMENT

This work was supported by the National Key R&D Program of China (2017YFA0506000 to C. S.), National Natural Science Foundation of China (81725020 to C. S.), and Science and Technology Commission of Shanghai Municipality (Grant 17XD1404700 to C. S.).

■ ABBREVIATIONS LIST

JAK, Janus kinase; HDAC, histone deacetylase; HSCT, hematopoietic stem cell transplantation; AML, acute myeloid leukemia; GVHD, graft versus host disease; IFIs, invasive fungal infections; STAT, signal transducers and activators of transcription; RA, rheumatoid arthritis; ZBG, zinc-binding group; HATU, 1-[Bis(dimethylamino)methylene]-1*H*-1,2,3-triazolo[4,5-b]pyridinium3-oxid hexafluorophosphate; DIPEA, *N,N*-Diisopropylethylamine; DMF, dimethylformamide; MIC, minimum inhibitory concentration; FIC, fractional inhibitory concentration; FLC, fluconazole; TGI, tumor growth inhibition; SCID, severe combined immune deficiency; ICR, Institute of Cancer Research; SD: Sprague-Dawley; CFU, colony-forming units; PI, propidium iodide; MST, median survival time; PK, pharmacokinetic.

■ REFERENCES

1. Pagano, L.; Caira, M.; Candoni, A.; Offidani, M.; Fianchi, L.; Martino, B.; Pastore, D.; Picardi, M.; Bonini, A.; Chierichini, A.; Fanci, R.; Caramatti, C.; Invernizzi, R.; Mattei, D.; Mitra, M. E.; Melillo, L.; Aversa, F.; Van Lint, M. T.; Falcucci, P.; Valentini, C. G.; Girmenia, C.; Nosari, A. The epidemiology of fungal

infections in patients with hematologic malignancies: the SEIFEM-2004 study. *Haematologica* **2006**, *91*, 1068-1075.

2. Pophali, P. A.; Patnaik, M. M. The role of new tyrosine kinase inhibitors in chronic myeloid leukemia. *Cancer J.* **2016**, *22*, 40-50.

3. Laurence, A.; Pesu, M.; Silvennoinen, O.; O'Shea, J. JAK kinases in health and disease: an update. *Open Rheumatol. J.* **2012**, *6*, 232-244.

4. O'Shea, J. J.; Plenge, R. JAK and STAT signaling molecules in immunoregulation and immune-mediated disease. *Immunity* **2012**, *36*, 542-550.

5. Shuai, K.; Liu, B. Regulation of JAK-STAT signalling in the immune system. *Nat. Rev. Immunol.* **2003**, *3*, 900-911.

6. Clark, J. D.; Flanagan, M. E.; Telliez, J. B. Discovery and development of janus kinase (JAK) inhibitors for inflammatory diseases. *J. Med. Chem.* **2014**, *57*, 5023-5038.

7. Kontzias, A.; Kotlyar, A.; Laurence, A.; Changelian, P.; O'Shea, J. J. Jakinibs: a new class of kinase inhibitors in cancer and autoimmune disease. *Curr. Opin. Pharmacol.* **2012**, *12*, 464-470.

8. Vainchenker, W.; Constantinescu, S. N. JAK/STAT signaling in hematological malignancies. *Oncogene* **2013**, *32*, 2601-2613.

9. Kaur, K.; Kalra, S.; Kaushal, S. Systematic review of tofacitinib: a new drug for the management of rheumatoid arthritis. *Clin. Ther.* **2014**, *36*, 1074-1086.

10. Plosker, G. L. Ruxolitinib: a review of its use in patients with myelofibrosis. *Drugs* **2015**, *75*, 297-308.

11. Buchert, M.; Burns, C. J.; Ernst, M. Targeting JAK kinase in solid tumors: emerging opportunities and challenges. *Oncogene* **2016**, *35*, 939-951.

12. Meyer, S. C. Mechanisms of resistance to JAK2 inhibitors in myeloproliferative neoplasms. *Hematol. Oncol. Clin. North Am.* **2017**, *31*, 627-642.

13. Bhagwat, N.; Levine, R. L.; Koppikar, P. Sensitivity and resistance of JAK2 inhibitors to myeloproliferative neoplasms. *Int. J. Hematol.* **2013**, *97*, 695-702.

14. Santos, F. P.; Verstovsek, S. What is next beyond janus kinase 2 inhibitors for primary myelofibrosis? *Curr. Opin. Hematol.* **2013**, *20*, 123-129.

15. Choong, M. L.; Pecquet, C.; Pendharkar, V.; Diaconu, C. C.; Yong, J. W.; Tai, S. J.; Wang, S. F.; Defour, J. P.; Sangthongpitag, K.; Villeval, J. L.; Vainchenker, W.; Constantinescu, S. N.; Lee, M. A. Combination treatment for myeloproliferative neoplasms using JAK and pan-class I PI3K inhibitors. *J. Cell. Mol. Med.* **2013**, *17*, 1397-1409.

16. Waibel, M.; Solomon, V. S.; Knight, D. A.; Ralli, R. A.; Kim, S. K.; Banks, K. M.; Vidacs, E.; Virely, C.; Sia, K. C.; Bracken, L. S.; Collins-Underwood, R.; Drenberg, C.; Ramsey, L. B.; Meyer, S. C.; Takiguchi, M.; Dickins, R. A.; Levine, R.; Ghysdael, J.; Dawson, M. A.; Lock, R. B.; Mullighan, C. G.; Johnstone, R. W. Combined targeting of JAK2 and Bcl-2/Bcl-xL to cure mutant JAK2-driven malignancies and overcome acquired resistance to JAK2 inhibitors. *Cell Rep.* **2013**, *5*, 1047-1059.

17. William, A. D.; Lee, A. C.; Goh, K. C.; Blanchard, S.; Poulsen, A.; Teo, E. L.; Nagaraj, H.; Lee, C. P.; Wang, H.; Williams, M.; Sun, E. T.; Hu, C.; Jayaraman, R.; Pasha, M. K.; Ethirajulu, K.; Wood, J. M.; Dymock, B. W. Discovery of kinase

spectrum selective macrocycle (16E)-14-methyl-20-oxa-5,7,14,26-tetraazatetracyclo[19.3.1.1(2,6).1(8,12)]heptaco sa-1(25),2(26),3,5,8(27),9,11,16,21,23-decaene (SB1317/TG02), a potent inhibitor of cyclin dependent kinases (CDKs), Janus kinase 2 (JAK2), and fms-like tyrosine kinase-3 (FLT3) for the treatment of cancer. *J. Med. Chem.* **2012**, *55*, 169-196.

18. William, A. D.; Lee, A. C.; Blanchard, S.; Poulsen, A.; Teo, E. L.; Nagaraj, H.; Tan, E.; Chen, D.; Williams, M.; Sun, E. T.; Goh, K. C.; Ong, W. C.; Goh, S. K.; Hart, S.; Jayaraman, R.; Pasha, M. K.; Ethirajulu, K.; Wood, J. M.; Dymock, B. W. Discovery of the macrocycle 11-(2-pyrrolidin-1-yl-ethoxy)-14,19-dioxa-5,7,26-triaza-tetracyclo[19.3.1.1(2,6). 1(8,12)]heptacosa-1(25),2(26),3,5,8,10,12(27),16,21,23-decaene (SB1518), a potent Janus kinase 2/fms-like tyrosine kinase-3 (JAK2/FLT3) inhibitor for the treatment of myelofibrosis and lymphoma. *J. Med. Chem.* **2011**, *54*, 4638-4658.

19. Conway, S. J.; Woster, P. M.; Shen, J. K.; Georg, G.; Wang, S. Epigenetics: novel therapeutics targeting epigenetics. *J. Med. Chem.* **2015**, *58*, 523-524.

20. Ververis, K.; Hiong, A.; Karagiannis, T. C.; Licciardi, P. V. Histone deacetylase inhibitors (HDACIs): multitargeted anticancer agents. *Biol.: Targets Ther.* **2013**, *7*, 47-60.

21. Mann, B. S.; Johnson, J. R.; Cohen, M. H.; Justice, R.; Pazdur, R. FDA approval summary: vorinostat for treatment of advanced primary cutaneous T-cell lymphoma. *Oncologist* **2007**, *12*, 1247-1252.

22. Bailey, H.; Stenehjem, D. D.; Sharma, S. Panobinostat for the treatment of

multiple myeloma: the evidence to date. *J. Blood Med.* **2015**, *6*, 269-276.

23. Manal, M.; Chandrasekar, M. J.; Gomathi Priya, J.; Nanjan, M. J. Inhibitors of histone deacetylase as antitumor agents: a critical review. *Bioorg. Chem.* **2016**, *67*, 18-42.

24. Ganesan, A. Multitarget drugs: an epigenetic epiphany. *ChemMedChem* **2016**, *11*, 1227-1241.

25. Anighoro, A.; Bajorath, J.; Rastelli, G. Polypharmacology: challenges and opportunities in drug discovery. *J. Med. Chem.* **2014**, *57*, 7874-7887.

26. Peters, J. U. Polypharmacology - foe or friend? *J. Med. Chem.* **2013**, *56*, 8955-8971.

27. Meyer, S. C.; Levine, R. L. Molecular pathways: molecular basis for sensitivity and resistance to JAK kinase inhibitors. *Clin. Cancer Res.* **2014**, *20*, 2051-2059.

28. Yao, L.; Mustafa, N.; Tan, E. C.; Poulsen, A.; Singh, P.; Duong-Thi, M. D.; Lee, J. X. T.; Ramanujulu, P. M.; Chng, W. J.; Yen, J. J. Y.; Ohlson, S.; Dymock, B. W. Design and synthesis of ligand efficient dual inhibitors of janus kinase (JAK) and histone deacetylase (HDAC) based on ruxolitinib and vorinostat. *J. Med. Chem.* **2017**, *60*, 8336-8357.

29. Yang, E. G.; Mustafa, N.; Tan, E. C.; Poulsen, A.; Ramanujulu, P. M.; Chng, W. J.; Yen, J. J.; Dymock, B. W. Design and synthesis of janus kinase 2 (JAK2) and histone deacetlyase (HDAC) bispecific inhibitors based on pacritinib and evidence of dual pathway inhibition in hematological cell lines. *J. Med. Chem.* **2016**, *59*, 8233-8262.

30. Dong, G.; Chen, W.; Wang, X.; Yang, X.; Xu, T.; Wang, P.; Zhang, W.; Rao, Y.;

Miao, C.; Sheng, C. Small molecule inhibitors simultaneously targeting cancer metabolism and epigenetics: discovery of novel nicotinamide phosphoribosyltransferase (NAMPT) and histone deacetylase (HDAC) dual inhibitors. *J. Med. Chem.* **2017**, *60*, 7965-7983.

31. He, S.; Dong, G.; Wang, Z.; Chen, W.; Huang, Y.; Li, Z.; Jiang, Y.; Liu, N.; Yao, J.; Miao, Z.; Zhang, W.; Sheng, C. Discovery of novel multiacting topoisomerase I/II and histone deacetylase inhibitors. *ACS Med. Chem. Lett.* **2015**, *6*, 239-243.

32. Zhuang, C.; Miao, Z.; Wu, Y.; Guo, Z.; Li, J.; Yao, J.; Xing, C.; Sheng, C.; Zhang, W. Double-edged swords as cancer therapeutics: novel, orally active, small molecules simultaneously inhibit p53-MDM2 interaction and the NF-kappaB pathway. *J. Med. Chem.* **2014**, *57*, 567-577.

33. Noronha, G.; Mak, C. C.; Cao, J.; Renick, J.; Mcpherson, A.; Zeng, B.; Pathak, V. P.; Lohse, D. L.; Hood, J. D.; Soll, R. M. Bi-aryl Meta-pyrimidine Inhibitors of Kinases. U.S. Patent 8,604,042, Dec. 10, 2013.

34. Gryder, B. E.; Sodji, Q. H.; Oyelere, A. K. Targeted cancer therapy: giving histone deacetylase inhibitors all they need to succeed. *Future Med. Chem.* **2012**, *4*, 505-524.

35. Burns, C. J.; Bourke, D. G.; Andrau, L.; Bu, X.; Charman, S. A.; Donohue, A. C.; Fantino, E.; Farrugia, M.; Feutrill, J. T.; Joffe, M.; Kling, M. R.; Kurek, M.; Nero, T. L.; Nguyen, T.; Palmer, J. T.; Phillips, I.; Shackleford, D. M.; Sikanyika, H.; Styles, M.; Su, S.; Treutlein, H.; Zeng, J.; Wilks, A. F. Phenylaminopyrimidines as inhibitors of Janus kinases (JAKs). *Bioorg. Med. Chem. Lett.* **2009**, *19*, 5887-5892.

36. Tiwari, S.; Thakur, R.; Shankar, J. Role of heat-shock proteins in cellular function and in the biology of fungi. *Biotechnol. Res. Int.* **2015**, *2015*, 132635.

37. Smith, W. L.; Edlind, T. D. Histone deacetylase inhibitors enhance Candida albicans sensitivity to azoles and related antifungals: correlation with reduction in CDR and ERG upregulation. *Antimicrob. Agents Chemother.* **2002**, *46*, 3532-3539.

38. Mai, A.; Rotili, D.; Massa, S.; Brosch, G.; Simonetti, G.; Passariello, C.; Palamara, A. T. Discovery of uracil-based histone deacetylase inhibitors able to reduce acquired antifungal resistance and trailing growth in Candida albicans. *Bioorg. Med. Chem. Lett.* **2007**, *17*, 1221-1225.

39. Li, X.; Cai, Q.; Mei, H.; Zhou, X.; Shen, Y.; Li, D.; Liu, W. The Rpd3/Hda1 family of histone deacetylases regulates azole resistance in Candida albicans. *J. Antimicrob. Chemother.* **2015**, *70*, 1993-2003.

40. Xu, Y.; Wang, Y.; Yan, L.; Liang, R. M.; Dai, B. D.; Tang, R. J.; Gao, P. H.; Jiang, Y. Y. Proteomic analysis reveals a synergistic mechanism of fluconazole and berberine against fluconazole-resistant Candida albicans: endogenous ROS augmentation. *J. Proteome Res.* **2009**, *8*, 5296-5304.

41. Odds, F. C. Synergy, antagonism, and what the chequerboard puts between them. *J. Antimicrob. Chemother.* **2003**, *52*, 1.

42. Millard, C. J.; Watson, P. J.; Celardo, I.; Gordiyenko, Y.; Cowley, S. M.; Robinson, C. V.; Fairall, L.; Schwabe, J. W. Class I HDACs share a common mechanism of regulation by inositol phosphates. *Mol. Cell* **2013**, *51*, 57-67.

43. Dugan, B. J.; Gingrich, D. E.; Mesaros, E. F.; Milkiewicz, K. L.; Curry, M. A.;

Zulli, A. L.; Dobrzanski, P.; Serdikoff, C.; Jan, M.; Angeles, T. S.; Albom, M. S.; Mason, J. L.; Aimone, L. D.; Meyer, S. L.; Huang, Z.; Wells-Knecht, K. J.; Ator, M. A.; Ruggeri, B. A.; Dorsey, B. D. A selective, orally bioavailable 1,2,4-triazolo[1,5-a]pyridine-based inhibitor of Janus kinase 2 for use in anticancer therapy: discovery of CEP-33779. *J. Med. Chem.* **2012**, *55*, 5243-5254.

44. Butler, K. V.; Kalin, J.; Brochier, C.; Vistoli, G.; Langley, B.; Kozikowski, A. P. Rational design and simple chemistry yield a superior, neuroprotective HDAC6 inhibitor, tubastatin A. *J. Am. Chem. Soc.* **2010**, *132*, 10842-10846.

45. Santo, L.; Hideshima, T.; Kung, A. L.; Tseng, J. C.; Tamang, D.; Yang, M.; Jarpe, M.; van Duzer, J. H.; Mazitschek, R.; Ogier, W. C.; Cirstea, D.; Rodig, S.; Eda, H.; Scullen, T.; Canavese, M.; Bradner, J.; Anderson, K. C.; Jones, S. S.; Raje, N. Preclinical activity, pharmacodynamic, and pharmacokinetic properties of a selective HDAC6 inhibitor, ACY-1215, in combination with bortezomib in multiple myeloma. *Blood* **2012**, *119*, 2579-2589.

46. Malvaez, M.; McQuown, S. C.; Rogge, G. A.; Astarabadi, M.; Jacques, V.; Carreiro, S.; Rusche, J. R.; Wood, M. A. HDAC3-selective inhibitor enhances extinction of cocaine-seeking behavior in a persistent manner. *Proc. Natl. Acad. Sci. U. S. A.* **2013**, *110*, 2647-2652.

47. Duan, W.; Li, J.; Inks, E. S.; Chou, C. J.; Jia, Y.; Chu, X.; Li, X.; Xu, W.; Zhang, Y. Design, synthesis, and antitumor evaluation of novel histone deacetylase inhibitors equipped with a phenylsulfonylfuroxan module as a nitric oxide donor. *J. Med. Chem.* **2015**, *58*, 4325-4338.

48. Yoon, K. B.; Cho, S. Y.; An, S. J.; Park, K. R.; Lee, H. J.; Yoon, H. S.; Lee, S. M.; Kim, Y. C.; Han, S. Y. Characterization of the aminopyridine derivative KRC-180 as a JAK2 inhibitor. *Oncol. Lett.* **2017**, *14*, 1347-1354.

49. Mathe, L.; Van Dijck, P. Recent insights into Candida albicans biofilm resistance mechanisms. *Curr. Genet.* **2013**, *59*, 251-264.

50. Vila, T. V.; Ishida, K.; de Souza, W.; Prousis, K.; Calogeropoulou, T.; Rozental, S. Effect of alkylphospholipids on Candida albicans biofilm formation and maturation. *J. Antimicrob. Chemother.* **2013**, *68*, 113-125.

51. Jiang, Z.; Liu, N.; Hu, D.; Dong, G.; Miao, Z.; Yao, J.; He, H.; Jiang, Y.; Zhang, W.; Wang, Y.; Sheng, C. The discovery of novel antifungal scaffolds by structural simplification of the natural product sampangine. *Chem. Commun.* **2015**, *51*, 14648-14651.

52. Pierce, C. G.; Uppuluri, P.; Tristan, A. R.; Wormley, F. L., Jr.; Mowat, E.; Ramage, G.; Lopez-Ribot, J. L. A simple and reproducible 96-well plate-based method for the formation of fungal biofilms and its application to antifungal susceptibility testing. *Nat. Protoc.* **2008**, *3*, 1494-1500.

53. Li, X.; Guo, H.; Duan, H.; Yang, Y.; Meng, J.; Liu, J.; Wang, C.; Xu, H. Improving chemotherapeutic efficiency in acute myeloid leukemia treatments by chemically synthesized peptide interfering with CXCR4/CXCL12 axis. *Sci. Rep.* **2015**, *5*, 16228.

54. Wang, X.; Lin, Q.; Lv, F.; Liu, N.; Xu, Y.; Liu, M.; Chen, Y.; Yi, Z. LG-362B targets PML-RARalpha and blocks ATRA resistance of acute promyelocytic leukemia.

Leukemia **2016**, *30*, 1465-1474.

55. Quan, H.; Cao, Y. Y.; Xu, Z.; Zhao, J. X.; Gao, P. H.; Qin, X. F.; Jiang, Y. Y. Potent in vitro synergism of fluconazole and berberine chloride against clinical isolates of Candida albicans resistant to fluconazole. *Antimicrob. Agents Chemother.* **2006**, *50*, 1096-1099.

Table of Contents Graphic